2. Materials and methods

2.1. Cells

A human monolayer cell line 293T [19] was cultured in Eagle's MEM supplemented with 10% heat-inactivated FBS (hiFBS). A cynomolgus macaque (CyM) lymphocyte cell line HSC-F [20] and a rhesus monkey (RhM) lymphocyte cell line HSR5.4S1 [21] were maintained in RPMI1640 containing 10% hiFBS (for HSR5.4S1, 50 units/mL of IL-2 (AbD Serotec) were added). Human MT4/CCR5 cells (MT4 cells stably expressing CCR5) were maintained RPMI1640 containing 10% hiFBS and 200 μg/mL hyglomycine (Sigma–Aldrich).

2.2. Transfection, RT assays and infection

Virus stocks were prepared by transfection of 293T cells with viral clones using the calcium phosphate co-precipitation method [22]. On day 2 post-transfection, culture supernatants were collected and stored at −80 °C until use. Virion-associated RT activity was measured as described previously [23]. HSC-F cells were infected with an equal amount of virus preparations in the presence of IL-2. For infection of MT4/CCR5 cells, the spinoculation method [24] was used. Virus replication was monitored by RT activity in the culture supernatants, and viral growth potentials were evaluated by the peak day of virus production or by the level of virus production on the peak day.

2.3. Plasmid DNAs

Construction of pHIV-1mt clones designated 5R and 562 has been previously described [14,16]. Proviral clones derived from adapted viruses were generated by PCR as described previously [14]. Two rounds of adaptation experiments independently performed are outlined in Figs. 1–4, and their details are described below. Introduction of genetic substitutions was performed by the QuickChange site-directed mutagenesis kit (Agilent Technologies).

2.4. First adaptation experiment

As indicated in Fig. 1, to construct molecular clones of adapted viruses from 5R and 562, CyM HSC-F cells were infected with the culture supernatants collected from long-term cultures. On day 9 post-infection, genomic DNA was extracted from cells, and integrated proviruses were amplified as two overlapping fragments by PCR as described previously [14]. To generate molecular clones that exhibit phenotypes of adapted viruses, we first introduced 3′ half genomes (*Eco*RI site in Vpr to *Sph*I site at 3′ end of the genome) from adapted 5R (5RA) and 562 (562A) viruses into 5R, and the resultant constructs were designated p5R/5RA3′ and p5R/562A3′, respectively. Virus stocks were prepared from 293T cells transfected with p5R/5RA3′ or p5R/562A3′, and inoculated into HSC-F cells. Virus replication was monitored by RT activity released into the culture supernatant. A molecular clone that grows best was selected for 5RA and 562A (p5R/5RA3′-14 and p5R/562A3′-3, respectively). Then, 5′ half genomes (*Aat*II site at the 5′ end of the genome to *Eco*RI site in Vpr) of adapted viruses (5RA5′ and 562A5′) were introduced into the selected clone (p5R/562A3′-3), and the resultant constructs were designated p5RA5′/562A3′-3 and p562A5′/562A3′-3, respectively. Proviral clones with the best replication potential were selected as described above. Finally, proviral clones that have a full-length viral genome derived from adapted 5R and 562 viruses were constructed, and designated MN4 and MN5, respectively (see Fig. 2 for their genome structures).

2.5. Second adaptation experiment

As indicated in Fig. 4, HSC-F (1×10^6) and RhM HSR5.4S1 cells (3×10^6) were infected with 5R or 562 viruses prepared from transfected 293T cells to obtain adapted viruses. Half of the culture medium (5 mL) was replaced every 3 days. Fresh HSC-F (1×10^6) and HSR5.4S1 cells (3×10^6) were added in each long-term culture on day 28 post-infection. Half of the culture medium (5 mL) was replaced every 3 days, and harvested supernatants were stored at −80 °C. HSC-F cells were infected with supernatants collected on day 33 post-infection from 5R- or 562-infected HSC-F long-term cultures. On day 9 and 12 post-infection, genomic DNA was extracted from infected cells. For HSR5.4S1 cultures, supernatants collected from 5R- and 562-infected cultures on day 39 and 42 post-infection, respectively, were inoculated into fresh HSR5.4S1 cells. On day 8 and 11 post-infection, genomic DNA was extracted from infected cultures. Amplification of integrated proviruses from genomic DNA and construction of proviral clones were carried out as described above. Viruses prepared from 293T cells transfected with these proviral clones were inoculated into HSC-F and HSR5.4S1 cells depending on which cells were used for long-term culture. Selection of viral clones with enhanced replication capability was carried out as described above.

3. Results

3.1. Mutations in Pol-IN or Env-gp120 are important for enhancement of pHIV-1mt replication in macaque cells

We previously reported that adapted viruses with enhanced growth potential emerged in prolonged cultures of 5R- or 562-infected macaque (CyM) cells [17]. Genomes of adapted viruses should have some genetic changes to augment their growth ability, and adapted viruses were expected to exist as a mass of viruses with distinct replication potential. To identify an adaptive mutation responsible for enhanced growth potential, it is necessary to construct proviral clones that exhibit a better-growing phenotype. Experimental details for construction are shown in Fig. 1. Of 72 proviral clones constructed, some of them (9 clones) did not produce virions in transfected 293T cells as determined by virion-associated RT activity or were not infectious for a CyM lymphocyte cell line HSC-F as well (16 clones). Finally, we have obtained molecular clones

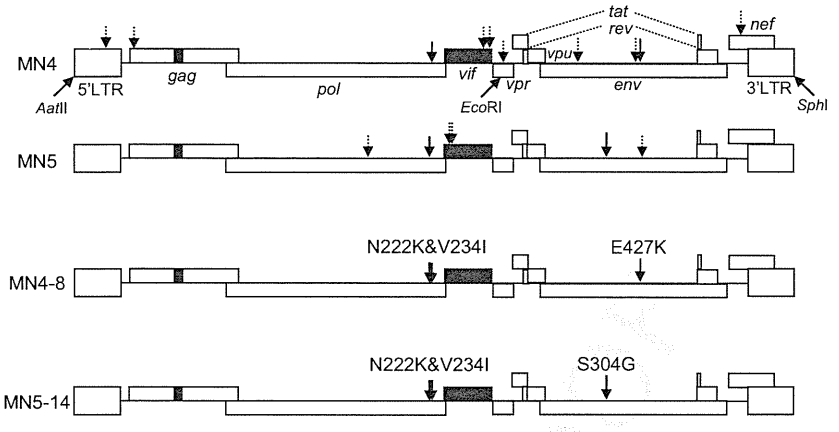

Virus	Genomes from adapted virus	Nucleotide change	Region	Amino acid change in the region
MN4	5' half	t453c	LTR	None
(derived from adapted 5R)	(MN4-5')	g823a	Matrix	E12K
		g4923a	**Pol-IN**	**V234I**
		g5611a	Vif	R171K
		g5693a	Vif	None
	3' half	g5944a	Vpr	None
	(MN4-3')	g6915a	Env-gp120 (V2)	None
		g7606a	Env-gp120 (V4)	E401K
		g7684a	**Env-gp120 (C4)**	**E427K**
		g9191a	Nef	V74I
MN5	5' half	a4049c	Reverse transcriptase	None
(derived from adapted 562)	(MN5-5')	**t4889a**	**Pol-IN**	**N222K**
		g5156a	Vif	None
		t5195a	Vif	None
	3' half	**a7318g**	**Env-gp120 (V3 loop)**	**S304G**
	(MN5-3')	c7812t	Env-gp120 (C5)	None

Fig. 2. Various mutations found in the first adaptation experiment. (Upper) Proviral genome structures of MN4, MN5, and their derivatives. Black areas show the regions derived from SIVmac239. Broken arrows show mutations that appeared during viral adaptation. Solid arrows indicate adaptive mutations in Pol-IN and Env-gp120 that enhance viral growth (Fig. 3). Out of the mutations present in MN4 and MN5, clones MN4-8 and MN5-14 carry the adaptive (growth-enhancing) mutations only. (Lower) Mutations associated with adaptation of 5R and 562 viruses to HSC-F cells. Bold letters show adaptive mutations that are responsible for enhancement of viral replication in cells. 5′ half indicates a fragment from *Aat*II at the 5′ end to *Eco*RI in *vpr* of the viral genome. 3′ half indicates a fragment from *Eco*RI in *vpr* to *Sph*I at the 3′ end of the viral genome.

MN4 and MN5 from adapted 5R and 562 viruses, respectively (Fig. 2).

To identify genetic changes acquired in genomes during virus adaptation, the entire genomes of MN4 and MN5 were sequenced. As shown in Fig. 2, MN4 and MN5 contained ten and six nucleotide substitutions, respectively. To examine the effect of these mutations on viral replication, each mutation was introduced into parental clones 5R and 562 as follows: (i) mutations in MN4 were introduced into 5R; (ii) mutations in 5′ half of MN5 genome were introduced into 5R (5′ half of 562 genome is identical to that of 5R (see Fig. 1A)); (iii) mutations in 3′ half of MN5 genome were introduced into 562. To construct positive control clones for viral growth (Fig. 3), we inserted a half of MN4 and MN5 genomes into the corresponding regions of 5R to generate full-length clones MN4-5′/5R, 5R/MN4-3′, MN5-5′/5R, and 5R/MN5-3′ (Fig. 2). Viruses were then prepared from 293T cells transfected with parental clones, positive controls, or test clones carrying each mutation, and inoculated into HSC-F cells (Fig. 3). MN4-5′ contains five genetic mutations (Fig. 2). Of the five clones examined, only the 5R carrying g4923a (V234I in IN) exhibited a similar growth kinetics to MN4-5′/5R (Fig. 3A). Growth kinetics of 5R carrying the other mutations were similar or slower relative to the parental clone 5R (Fig. 3A). MN4-3′ and MN5-5′ carry five and four nucleotide substitutions, respectively (Fig. 2). A clone that exhibits similar growth kinetics to 5R/MN4-3′ was 5R carrying g7684a

Please cite this article in press as: M. Nomaguchi, et al., Systemic biological analysis of the mutations in two distinct HIV-1mt genomes occurred during replication in macaque cells, Microbes and Infection (2013), http://dx.doi.org/10.1016/j.micinf.2013.01.005

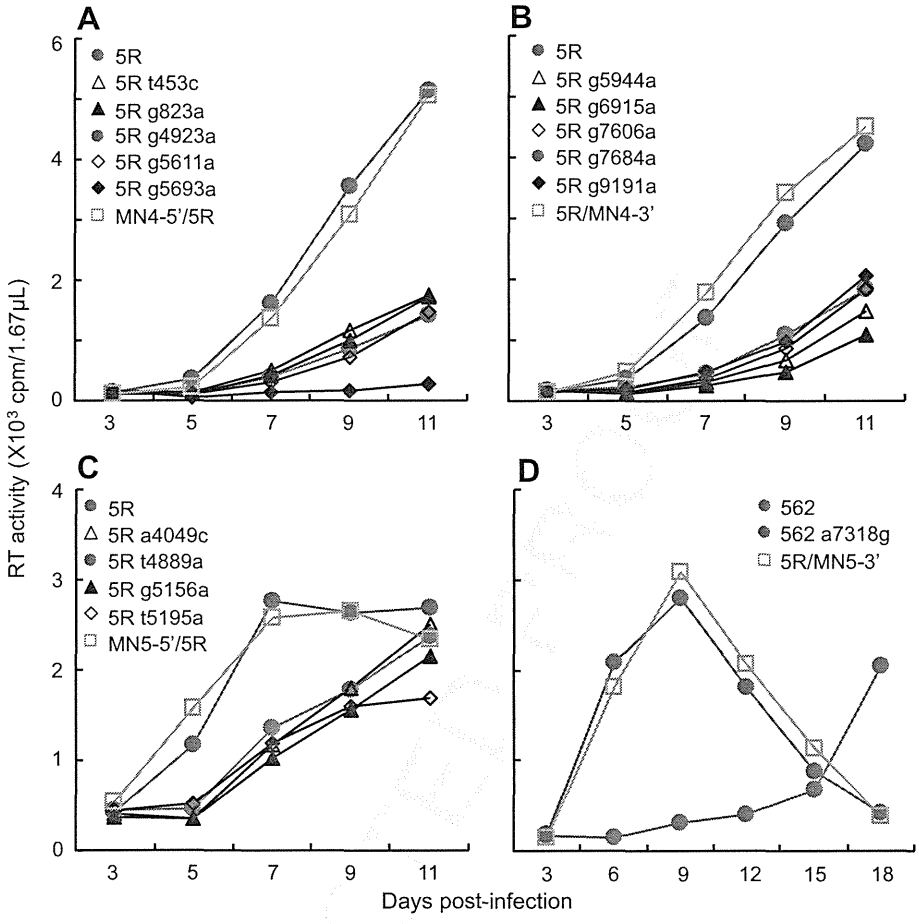

Fig. 3. Effect of individual mutations found in MN4 and MN5 on viral replication in HSC-F cells. Virus samples were prepared from 293T cells transfected with the indicated proviral clones, and inoculated into HSC-F cells (10^6) with an equal amount of viruses (A; 1.6×10^7 RT units, B; 8.5×10^6 RT units, C; 3.9×10^7 RT units, and D; 1.2×10^7 RT units). Proviral clones, MN4-5′/5R, 5R/MN4-3′, MN5-5′/5R, and 5R/MN5-3′, carry 5′ or 3′ half genomes of MN4 or MN5 in the context of 5R genome (Fig. 2). These clones served as positive controls. Virus replication was monitored by RT activity released into the culture supernatants.

(E427K in gp120) (Fig. 3B). 5R carrying t4889a (N222K in IN) showed a similar growth property with MN5-5′/5R (Fig. 3C). Two mutations (non-synonymous and synonymous) were found in MN5-3′ (Fig. 2), but only the non-synonymous mutation (a7318g, S304G in gp120) was tested. The viral clone 562 a7318g showed similar growth kinetics to those of 5R/MN5-3′ (Fig. 3D). In total, the growth-enhancing mutations were found only in *pol*-IN (V234I in 5R and N222K in 562) and *env*-gp120 (E427K in 5R and S304G in 562) regions despite the presence of mutations in the other regions.

3.2. Adaptive mutations in Pol-IN and 562 Env-gp120 are critical for augmentation of pHIV-1mt replication

Growth potential of both MN4 and MN5 obtained from adaptation of two distinct viruses was augmented by mutations in Pol-IN and Env-gp120 (Figs. 2 and 3). To clarify the requirements of adaptive mutations in these regions for enhancement of viral replication, we repeated the virus adaptation experiment (Fig. 4). Because it has been suggested that cellular environment is different between cell lines and affects outcome of virus adaptation [25], we used two distinct viruses (5R and 562) and two different macaque lymphocyte cell lines (CyM HSC-F and RhM HSR5.4S1) in this experiment. During long-term cultures of HSC-F and HSR5.4S1 cells infected with 5R or 562, adapted viruses emerged as judged by the growth property of viruses produced in the culture supernatants as previously described [17]. A number of proviral clones derived from adapted viruses were constructed similarly as above, and test viruses were prepared from transfected 293T cells. Viruses were then inoculated into HSC-F or HSR5.4S1 cells depending on which cells were used for adaptation. We selected proviral clones that show clearly enhanced viral replication in macaque cells, and sequenced their entire genomes. As shown in Fig. 4, of viral clones that bear 5′ half of genomes from adapted 5R, we selected four clones from HSC-F cells and one clone from HSR5.4S1 cells. All of them carried a genetic mutation in Pol-IN (D229E or F223Y) that enhances viral growth potential (Fig. 4B, note the peak day of virus production). Four adaptive mutations identified in Pol-IN (N222K, F223Y, D229E and V234I) were located in a narrow region of IN C-terminal domain (IN-CTD). On the other hand, none of viral clones carrying 3′ half of genomes from adapted 5R exhibited augmentation of viral

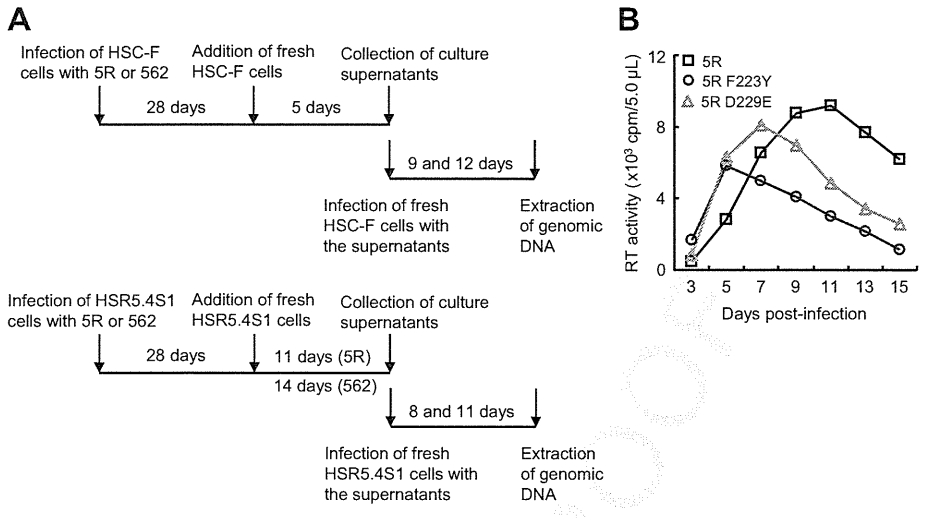

C

Virus/Macaque cells used for long-term culture	Half genome derived from adapted viruses	Number of clones examined for growth kinetics	Number of clones with enhanced viral growth	Adaptive mutations in IN-CTD and Env-gp120
5R/HSC-F	5'	39	4	IN-CTD D229E (4)
	3'	43	0	NA
5R/HSR5.4S1	5'	24	1	IN-CTD F223Y (1)
	3'	62	0	NA
562/HSC-F	5'	41	1	IN-CTD N222K (1)
	3'	16	13	V3 S304G (8) V1 G150R (2) C1 L124F (1) V1 N132K (1) V3 I307V (1)
562/HSR5.4S1	5'	27	0	NA
	3'	32	20	V3 S304G (9) V2 F174L (7) V1 L124F (1) V2 P181T (1) V3 G308E (1) V3 G310R (1)

Fig. 4. Various adaptive (growth-enhancing) mutations found in the second adaptation experiment. (A) Generation of molecular clones from adapted 5R and 562 viruses. Schedule of virus adaptation and the harvest of adapted viruses are shown. Cellular genomic DNA preparations for molecular cloning of viruses are indicated. For details, see Materials and methods. (B) Growth kinetics of Pol-IN mutants in HSC-F cells. Virus samples (3.5×10^6 RT units) were prepared from 293T cells transfected with the indicated proviral clones, and inoculated into CyM HSC-F (10^6). Virus replication was monitored by RT activity released into the culture supernatants. (C) Frequency of adaptive mutations in IN-CTD and Env-gp120. Number in parentheses refers to the number of clones carrying the indicated mutation. In total, all viral clones with enhanced growth potential were found to have adaptive mutations in IN-CTD or Env-gp120. NA, not applicable.

replication. This may imply that 5R has been already better adapted to HSC-F cells, since 5R has acquired mutations in *env* and LTR by virus adaptation within the cells [14]. In viral clones bearing 5′ half genome from adapted 562, one selected clone carried the same N222K mutation in IN-CTD as MN5. Enhanced growth potentials were noted for many clones that carry 3′ half genome from adapted 562. Around half of the selected clones carried S304G in Env-gp120 V3 loop, and the rest of clones carried adaptive (growth-enhancing) mutations in the C1, V1, V2, or V3 region of Env-gp120. Similar results with those in HSC-F cells were obtained in HSR5.4S1 cells (data not shown). The results described above indicate that adaptive mutations in IN-CTD and 562 Env-gp120 are critical for enhancement of viral growth potential in macaque cells.

3.3. Introduction of either single or double adaptive IN-CTD mutations (N222K and V234I) enhances viral growth both in macaque and human cells

Replication of two distinct pHIV-1mt was augmented by acquiring N222K or V234I in IN-CTD during virus adaptation in macaque cells (Figs. 2 and 3). To examine whether these adaptive mutations have an additive effect on viral replication, we constructed 5R carrying single (designated 5R N222K and 5R V234I) or double (designated 5R NKVI) mutations. We were also interested in determining the effect of the mutations on viral growth in human cells. Viruses prepared from transfected 293T cells were inoculated into HSC-F and human MT4/CCR5 cells. As shown in Fig. 5A, 5R NKVI exhibited similar growth kinetics in macaque HSC-

Please cite this article in press as: M. Nomaguchi, et al., Systemic biological analysis of the mutations in two distinct HIV-1mt genomes occurred during replication in macaque cells, Microbes and Infection (2013), http://dx.doi.org/10.1016/j.micinf.2013.01.005

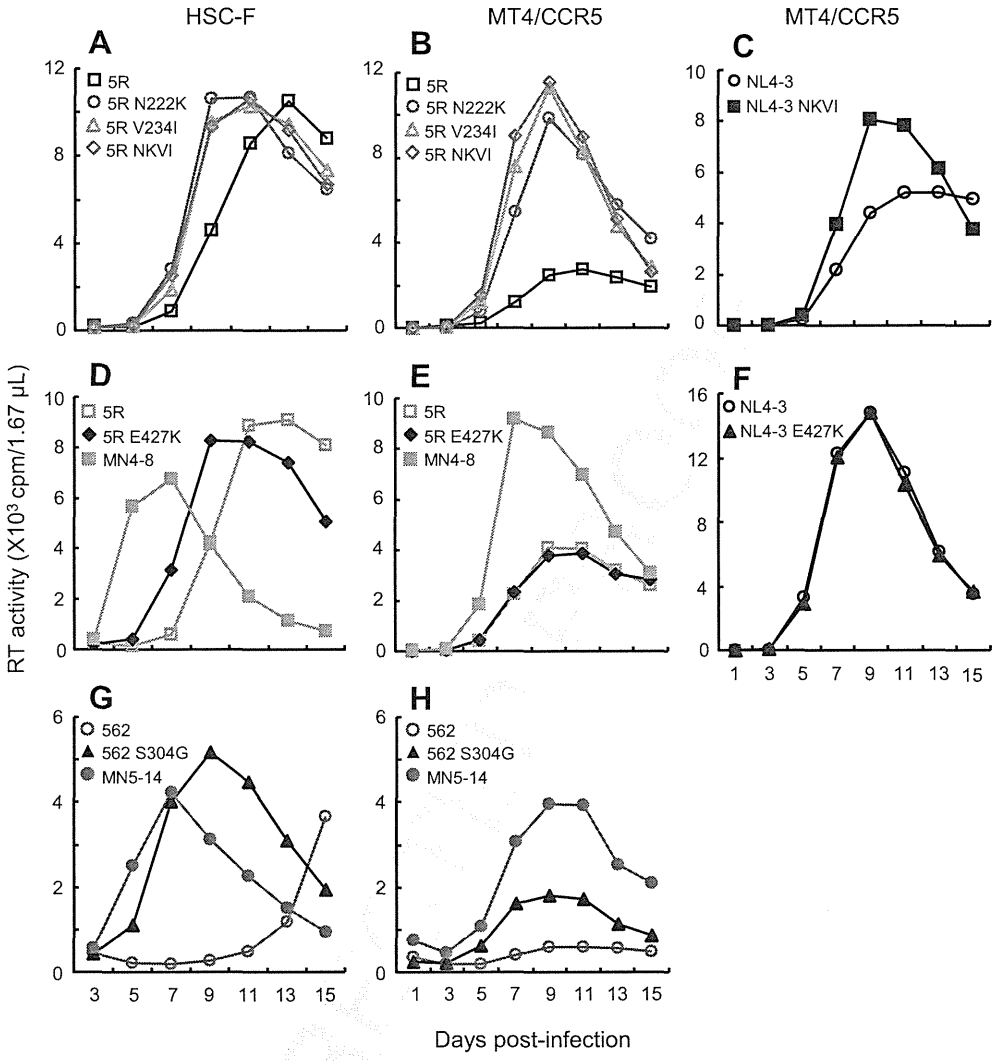

Fig. 5. Effect of adaptive mutations on viral replication. Growth kinetics in the indicated cell lines of various mutant viruses are presented. Virus samples were prepared from 293T cells transfected with the indicated proviral clones, and inoculated into CyM HSC-F (10^6) or spinoculated into human MT4/CCR5 (10^6) cells. Input viral amounts used were 1.0×10^7 RT units, 1.0×10^6 RT units, 1.1×10^5 RT units, 1.2×10^7 RT units, 1.0×10^6 RT units, 1.3×10^5 RT units, 1.2×10^7 RT units and 2.8×10^7 RT units for panels A, B, C, D, E, F, G and H, respectively. Virus replication was monitored by RT activity released into the culture supernatants. (A and B) Growth kinetics of 5R carrying single or double adaptive mutations in IN-CTD. 5R NKVI contains both N222K and V234I mutations. 5R served as a control. (C and F) Growth kinetics of NL4-3 viruses bearing IN NKVI (N222K and V234I) or Env E427K mutation. NL4-3 served as control. (D, E, G and H) Growth kinetics of various viruses carrying adaptive mutations. 5R and 562 served as controls.

F cells to those of 5R N222K and 5R V234I, and all these viruses grew better than 5R. Essentially the same results were obtained in human MT4/CCR5 cells (Fig. 5B). To determine whether the viral growth enhancement by adaptive mutations in IN-CTD is specific to pHIV-1mt, the mutational effect in the context of a standard HIV-1 clone NL4-3 was examined in MT4/CCR5 cells. As is clear in Fig. 5C, the adaptive mutations in IN-CTD also enhanced NL4-3 replication. Unexpectedly, we found that the four adaptive mutations in IN-CTD (Figs. 2 and 4) augment virion production independently of the IN authentic function (manuscript in preparation). In sum, these results show that adaptive mutations in IN-CTD augment growth potential of HIV-1, and that this effect is neither host-cell species-specific nor viral clone-specific.

3.4. E427K in 5R Env-gp120 promotes viral growth specifically in macaque cells, whereas enhancement of viral growth by S304G in 562 Env-gp120 is observed both in macaque and human cells

We constructed proviral clones that have both adaptive mutations in Pol-IN and Env-gp120 in anticipation of additive positive effects. Two mutations in Pol-IN (N222K and V234I) were introduced into clones 5R E427K and 562 S304G, which carry an adaptive mutation in Env-gp120, and designated MN4-8 and MN5-14, respectively (Fig. 2). Viruses prepared from transfected 293T cells were inoculated into HSC-F and MT4/CCR5 cells, and monitored for their growth kinetics (Fig. 5). 5R E427K exhibited rapid growth kinetics relative to 5R in HSC-F cells, but similar in MT4/CCR5 cells (Fig. 5D

Please cite this article in press as: M. Nomaguchi, et al., Systemic biological analysis of the mutations in two distinct HIV-1mt genomes occurred during replication in macaque cells, Microbes and Infection (2013), http://dx.doi.org/10.1016/j.micinf.2013.01.005

and E). To confirm this result, E427K was introduced into NL4-3 Env, which is the origin of 5R Env. NL4-3 carrying E427K showed similar growth kinetics to those of NL4-3 in MT4/CCR5 cells (Fig. 5F). Quite in contrast, the replication of 562 S304G was accelerated compared to that of 562 both in human and macaque cells (Fig. 5G and H). These results indicate that the effect of E427K mutation is host cell species-specific, whereas S304G shows the species-independent positive effect. Notably, E427K and S304G mutations were found to increase viral binding efficiency to CD4 and affinity to CCR5, respectively (manuscript in preparation). Growth potential of MN4-8 and MN5-14 was further enhanced both in macaque and human cells relative to 5R E427K and 562 S304G, respectively (Fig. 5), showing that combination of adaptive mutations in IN-CTD and Env-gp120 has an additive effect on viral replication (note the peak day of virus production).

3.5. Enhancement of viral growth by adaptive Env-gp120 mutations is dependent on the env *sequence context*

E427K in 5R and S304G in 562 were located in a distinct region within Env-gp120, C4 region and V3 loop, respectively. Alignment of Env-gp120 amino acid sequence of 5R and 562 indicated that the corresponding sites of E427K and S304G are E419K for 562 and S304G for 5R, respectively (Fig. 6A). Since functional relationship between C4 region and V3 loop for viral infection has been reported [26,27], we examined the effect of combination of adaptive mutations in these regions on viral growth. Proviral clones were generated by introducing S304G into 5R and 5R E427K (designated 5R S304G and 5R SGEK, respectively), and E419K into 562 and 562 S304G (designated 562 E419K and 562 SGEK, respectively). Viruses prepared from transfected 293T cells were inoculated into HSC-F cells, and monitored for their growth property. As shown in Fig. 6B and C, while enhancement of viral replication was again observed for 5R E427K and 562 S304G relative to 5R and 562, respectively, the growth of 5R S304G and 562 E419K was undetectable. Clones 5R SGEK and 562 SGEK somewhat restored their infectivity. These results show that the positive effect of adaptive mutations in Env-gp120 is sequence-specific. This is similar to the result in a previous report that the impact of one amino acid change within V3 loop on sensitivity to entry inhibitors is dependent on *env* context [28].

4. Discussion

In this study, we generated MN4 and MN5 clones with enhanced growth potential by virus adaptation in macaque cells. MN4 and MN5 have a number of nucleotide substitutions throughout their genomes (Fig. 2). Interestingly, only the mutations in IN-CTD and Env-gp120 were responsible for augmentation of viral replication (Figs. 2 and 3). In the second round of virus adaptation experiment using two distinct viruses and two different kinds of macaque cells, the mutations in IN-CTD and in 562 Env-gp120 were frequently found in the genomes of viral clones that exhibit rapid growth kinetics (Fig. 4). These results indicate that adaptive mutations in

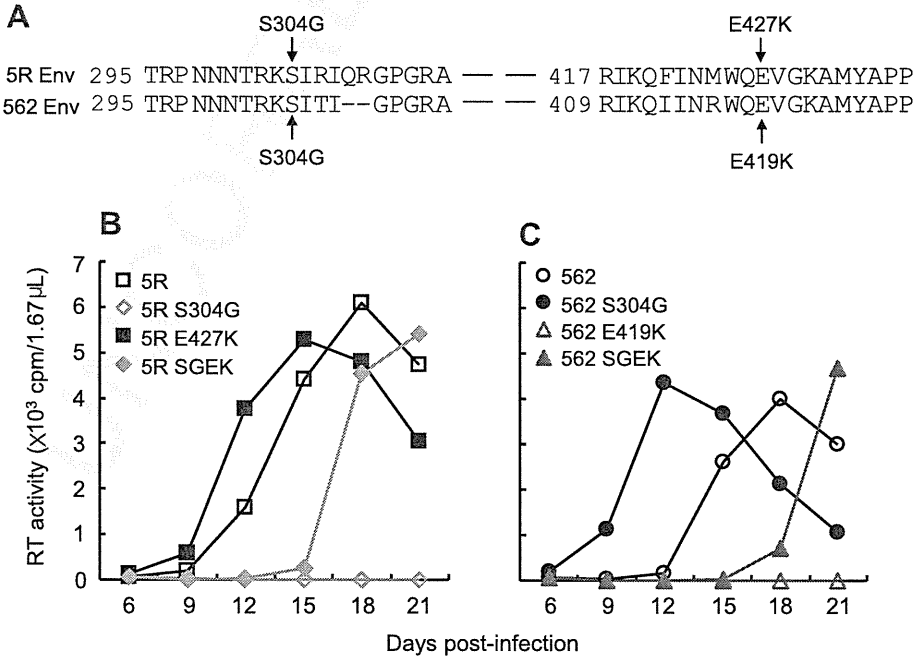

Fig. 6. Effect of combination of the adaptive mutations in Env-gp120 on viral replication. (A) Amino acid alignment of the regions close to adaptive mutations in 5R and 562. The corresponding sites to adaptive mutations in 5R and 562 are indicated. (B and C) Growth kinetics in HSC-F cells of 5R and 562 viruses carrying Env E419K/E427K and/or S304G mutation. Virus samples were prepared from 293T cells transfected with the indicated proviral clones, and inoculated into HSC-F cells (10^6) with an equal amount of viruses (1.0×10^7 RT units). 5R SGEK and 562 SGEK carry both S304G and E419K/E427K mutations. 5R and 562 served as controls. Virus replication was monitored by RT activity released into the culture supernatants.

Please cite this article in press as: M. Nomaguchi, et al., Systemic biological analysis of the mutations in two distinct HIV-1mt genomes occurred during replication in macaque cells, Microbes and Infection (2013), http://dx.doi.org/10.1016/j.micinf.2013.01.005

a narrow region of IN-CTD and in Env-gp120 are critical for growth-adaptation of pHIV-1mt in macaque cells. These results also suggest that pHIV-1mt may evolve in a certain direction to enhance their replication under uniform and strong restrictive environment in macaque cells. Notably, of the adaptive mutations examined, almost all were effective in both macaque and human cells with respect to promoting virus replication (Fig. 5).

In virus adaptation experiments, we obtained numerous proviral clones carrying the mutations in IN-CTD or S304G in 562, which exhibit enhanced growth potential (Figs. 2 and 4). Because genetic changes found in the other regions were different, the mutations came from different virus clones. Reason for the observed high frequency of adaptive IN-CTD and S304G mutations is presently unclear. Viruses may be apt to acquire the mutations in IN-CTD and Env-gp120 regions during adaptation by unknown mechanism. Alternatively, the rapid replication of mutant clones expanded the mutations in a mass of viruses, and resulted in their frequent selection. On the other hand, mutations in IN-CTD and S304G in 562 gp120 enhanced viral growth both in macaque and human cells (Fig. 5). These results indicate that the mutations are not relevant to evasion from the restriction factors responsible or critical for species-tropism. In fact, genetic alterations that influence viral replication were not found in *vif*, *gag*-CA, and *vpu*, which target APOBEC3G/F, CypA/TRIM5 proteins, and tetherin, respectively (Figs. 2 and 4). In this regard, it is interesting to note that replication efficiency of pHIV-1mt (5R and 562) is quite low in macaque cells [14,15]. Strong restriction of replication imposed by macaque cells may serve as a selective pressure on viruses during adaptation. Under this pressure, pHIV-1mt would have evolved to enhance growth ability itself, probably at a basal level, by acquiring the IN-CTD and gp120 mutations rather than to overcome the species barrier. HIV-1mt derivatives described in this report are still poorly infectious for CyM peripheral blood mononuclear cells (PBMCs) relative to the standard SIVmac and SHIV (chimera between SIVmac and HIV-1) clones. However, the enhancing effect of IN-CTD and Env-gp120 mutations was also observed in $CD8^+$ cell-depleted CyM PBMCs [29], confirming the results obtained in the cell lines. To further enhance growth potentials of HIV-1mt clones, it was found to be necessary to efficiently evade the species barrier [29,30]. Detailed functional and structural analyses of the mutations are required to elucidate the whole picture of the adaptive evolution described here. Studies in this direction are in progress in our laboratory.

In conclusion, we have demonstrated here that our adaptation system using virus-infected cells is a powerful tool to study virus replication and its underlying mechanism. We have readily and successfully identified the mutations, from mixtures of biologically insignificant and significant ones, that play a key role in viral replication, as also shown for SIVcpz (SIV isolated from chimpanzees) in human lymphoid tissue [31]. Since how viruses change their phenotypes is dependent on a power balance between viruses and cells, the combination of various primate lentiviruses (HIVs versus SIVs) and cells (human versus macaque) can produce different results upon adaptation. Information of adaptive mutations obtained from these experiments would be invaluable to learn and understand mechanisms for virus replication and evolution.

Acknowledgments

We thank Ms. Kazuko Yoshida for editorial assistance. This study is supported by a grant from the Ministry of Health, Labour and Welfare of Japan (Research on HIV/AIDS project no. H23-003).

References

[1] L.M. Mansky, H.M. Temin, Lower in vivo mutation rate of human immunodeficiency virus type 1 than that predicted from the fidelity of purified reverse transcriptase, J. Virol. 69 (1995) 5087–5094.
[2] D.N. Levy, G.M. Aldrovandi, O. Kutsch, G.M. Shaw, Dynamics of HIV-1 recombination in its natural target cells, Proc. Natl. Acad. Sci. U. S. A. 101 (2004) 4204–4209.
[3] J.M. Coffin, HIV population dynamics in vivo: implications for genetic variation, pathogenesis, and therapy, Science 267 (1995) 483–489.
[4] M.H. Malim, M. Emerman, HIV-1 sequence variation: drift, shift, and attenuation, Cell 104 (2001) 469–472.
[5] T. van Opijnen, B. Berkhout, The host environment drives HIV-1 fitness, Rev. Med. Virol. 15 (2005) 219–233.
[6] J.M. Carlson, Z.L. Brumme, HIV evolution in response to HLA-restricted CTL selection pressures: a population-based perspective, Microbes Infect. 10 (2008) 455–461.
[7] R.K. Holmes, M.H. Malim, K.N. Bishop, APOBEC-mediated viral restriction: not simply editing? Trends Biochem. Sci. 32 (2007) 118–128.
[8] J. Luban, Cyclophilin A, TRIM5, and resistance to human immunodeficiency virus type 1 infection, J. Virol. 81 (2007) 1054–1061.
[9] H. Huthoff, G.J. Towers, Restriction of retroviral replication by APOBEC3G/F and TRIM5alpha, Trends Microbiol. 16 (2008) 612–619.
[10] A. Tokarev, M. Skasko, K. Fitzpatrick, J. Guatelli, Antiviral activity of the interferon-induced cellular protein BST-2/tetherin, AIDS Res. Hum. Retroviruses 25 (2009) 1197–1210.
[11] S.L. Sawyer, M. Emerman, H.S. Malik, Ancient adaptive evolution of the primate antiviral DNA-editing enzyme APOBEC3G, PLoS Biol. 2 (2004) E275.
[12] S.L. Sawyer, L.I. Wu, M. Emerman, H.S. Malik, Positive selection of primate TRIM5alpha identifies a critical species-specific retroviral restriction domain, Proc. Natl. Acad. Sci. U. S. A. 102 (2005) 2832–2837.
[13] M.W. McNatt, T. Zang, T. Hatziioannou, M. Bartlett, I.B. Fofana, W.E. Johnson, S.J. Neil, P.D. Bieniasz, Species-specific activity of HIV-1 Vpu and positive selection of tetherin transmembrane domain variants, PLoS Pathog. 5 (2009) e1000300.
[14] K. Kamada, T. Igarashi, M.A. Martin, B. Khamsri, K. Hatcho, T. Yamashita, M. Fujita, T. Uchiyama, A. Adachi, Generation of HIV-1 derivatives that productively infect macaque monkey lymphoid cells, Proc. Natl. Acad. Sci. U. S. A. 103 (2006) 16959–16964.
[15] T. Igarashi, R. Iyengar, R.A. Byrum, A. Buckler-White, R.L. Dewar, C.E. Buckler, H.C. Lane, K. Kamada, A. Adachi, M.A. Martin, Human immunodeficiency virus type 1 derivative with 7% simian immunodeficiency virus genetic content is able to establish infections in pig-tailed macaques, J. Virol. 81 (2007) 11549–11552.
[16] T. Yamashita, N. Doi, A. Adachi, M. Nomaguchi, Growth ability in simian cells of monkey cell-tropic HIV-1 is greatly affected by downstream region of the vif gene, J. Med. Invest. 55 (2008) 236–240.
[17] M. Nomaguchi, N. Doi, K. Kamada, A. Adachi, Species barrier of HIV-1 and its jumping by virus engineering, Rev. Med. Virol. 18 (2008) 261–275.
[18] M. Kimura, Evolutionary rate at the molecular level, Nature 217 (1968) 624–626.

[19] J.S. Lebkowski, S. Clancy, M.P. Calos, Simian virus 40 replication in adenovirus-transformed human cells antagonizes gene expression, Nature 317 (1985) 169–171.
[20] H. Akari, T. Fukumori, S. Iida, A. Adachi, Induction of apoptosis in *Herpesvirus saimiri*-immortalized T lymphocytes by blocking interaction of CD28 with CD80/CD86, Biochem. Biophys. Res. Commun. 263 (1999) 352–356.
[21] N. Doi, S. Fujiwara, A. Adachi, M. Nomaguchi, Growth ability in various macaque cell lines of HIV-1 with simian cell-tropism, J. Med. Invest. 57 (2010) 284–292.
[22] A. Adachi, H.E. Gendelman, S. Koenig, T. Folks, R. Willey, A. Rabson, M.A. Martin, Production of acquired immunodeficiency syndrome-associated retrovirus in human and nonhuman cells transfected with an infectious molecular clone, J. Virol. 59 (1986) 284–291.
[23] R.L. Willey, D.H. Smith, L.A. Lasky, T.S. Theodore, P.L. Earl, B. Moss, D.J. Capon, M.A. Martin, In vitro mutagenesis identifies a region within the envelope gene of the human immunodeficiency virus that is critical for infectivity, J. Virol. 62 (1988) 139–147.
[24] U. O'Doherty, W.J. Swiggard, M.H. Malim, Human immunodeficiency virus type 1 spinoculation enhances infection through virus binding, J. Virol. 74 (2000) 10074–10080.
[25] T. van Opijnen, A. de Ronde, M.C. Boerlijst, B. Berkhout, Adaptation of HIV-1 depends on the host-cell environment, PLoS One 2 (2007) e271.
[26] A. Carrillo, L. Ratner, Human immunodeficiency virus type 1 tropism for T-lymphoid cell lines: role of the V3 loop and C4 envelope determinants, J. Virol. 70 (1996) 1301–1309.
[27] N.G. Hoffman, F. Seillier-Moiseiwitsch, J. Ahn, J.M. Walker, R. Swanstrom, Variability in the human immunodeficiency virus type 1 gp120 Env protein linked to phenotype-associated changes in the V3 loop, J. Virol. 76 (2002) 3852–3864.
[28] M.A. Lobritz, A.J. Marozsan, R.M. Troyer, E.J. Arts, Natural variation in the V3 crown of human immunodeficiency virus type 1 affects replicative fitness and entry inhibitor sensitivity, J. Virol. 81 (2007) 8258–8269.
[29] A. Saito, M. Nomaguchi, S. Iijima, A. Kuroishi, T. Yoshida, Y.J. Lee, T. Hayakawa, K. Kono, E.E. Nakayama, T. Shioda, Y. Yasutomi, A. Adachi, T. Matano, H. Akari, Improved capacity of a monkey-tropic HIV-1 derivative to replicate in cynomolgus monkeys with minimal modifications, Microbes Infect. 13 (2011) 58–64.
[30] M. Nomaguchi, M. Yokoyama, K. Kono, E.E. Nakayama, T. Shioda, A. Saito, H. Akari, Y. Yasutomi, T. Matano, H. Sato, A. Adachi, Gag-CA Q110D mutation elicits TRIM-independent enhancement of HIV-1mt replication in macaque cells, Microbes Infect. 15 (2013) 56–65.
[31] F. Bibollet-Ruche, A. Heigele, B.F. Keele, J.L. Easlick, J.M. Decker, J. Takehisa, G. Learn, P.M. Sharp, B.H. Hahn, F. Kirchhoff, Efficient SIVcpz replication in human lymphoid tissue requires viral matrix protein adaptation, J. Clin. Invest. 122 (2012) 1644–1652.
[32] M. Kawamura, T. Ishizaki, A. Ishimoto, T. Shioda, T. Kitamura, A. Adachi, Growth ability of human immunodeficiency virus type 1 auxiliary gene mutants in primary blood macrophage cultures, J. Gen. Virol. 75 (1994) 2427–2431.

Please cite this article in press as: M. Nomaguchi, et al., Systemic biological analysis of the mutations in two distinct HIV-1mt genomes occurred during replication in macaque cells, Microbes and Infection (2013), http://dx.doi.org/10.1016/j.micinf.2013.01.005

Arch Virol
DOI 10.1007/s00705-013-1618-6

ORIGINAL ARTICLE

Dynamics of cellular immune responses in the acute phase of dengue virus infection

Tomoyuki Yoshida · Tsutomu Omatsu · Akatsuki Saito · Yuko Katakai · Yuki Iwasaki · Terue Kurosawa · Masataka Hamano · Atsunori Higashino · Shinichiro Nakamura · Tomohiko Takasaki · Yasuhiro Yasutomi · Ichiro Kurane · Hirofumi Akari

Received: 13 June 2012 / Accepted: 12 December 2012

Abstract In this study, we examined the dynamics of cellular immune responses in the acute phase of dengue virus (DENV) infection in a marmoset model. Here, we found that DENV infection in marmosets greatly induced responses of CD4/CD8 central memory T and NKT cells. Interestingly, the strength of the immune response was greater in animals infected with a dengue fever strain than in those infected with a dengue hemorrhagic fever strain of DENV. In contrast, when animals were re-challenged with the same DENV strain used for primary infection, the neutralizing antibody induced appeared to play a critical role in sterilizing inhibition against viral replication, resulting in strong but delayed responses of CD4/CD8 central memory T and NKT cells. The results in this study may help to better understand the dynamics of cellular and humoral immune responses in the control of DENV infection.

T. Yoshida and T. Omatsu contributed equally to this study.

Electronic supplementary material The online version of this article (doi:10.1007/s00705-013-1618-6) contains supplementary material, which is available to authorized users.

T. Yoshida · Y. Iwasaki · T. Kurosawa · M. Hamano · Y. Yasutomi · H. Akari
Tsukuba Primate Research Center, National Institute of Biomedical Innovation, 1-1 Hachimandai, Tsukuba, Ibaraki 305-0843, Japan

T. Yoshida (✉) · A. Saito · A. Higashino · H. Akari (✉)
Center for Human Evolution Modeling Research, Primate Research Institute, Kyoto University, Inuyama, Aichi 484-8506, Japan
e-mail: yoshida.tomoyuki.4w@kyoto-u.ac.jp

H. Akari
e-mail: akari.hirofumi.5z@kyoto-u.ac.jp

Introduction

Dengue virus (DENV) causes the most prevalent arthropod-borne viral infections in the world [29]. Infection with one of the four serotypes of DENV can lead to dengue fever (DF) and sometimes to fatal dengue hemorrhagic fever (DHF) or dengue shock syndrome (DSS) [12]. The serious diseases are more likely to develop after secondary infection with a serotype of DENV that is different from that of the primary infection. Infection with DENV induces a high-titered neutralizing antibody response that can provide long-term immunity to the homologous DENV serotype, while the effect of the antibody on the heterologous serotypes is transient [22]. On the other hand, enhanced pathogenicity after secondary DENV infection appears to be explained by antibody-dependent enhancement (ADE). Mouse and monkey experiments have shown that subneutralizing levels of DENV-specific antibodies actually enhance infection [1, 6, 11]. Thus, the development of an effective tetravalent dengue vaccine is considered to be an important public-health priority. Recently, several DENV vaccine candidates have undergone clinical trials, and most of them target the induction of neutralizing antibodies [20].

T. Omatsu · T. Takasaki · I. Kurane
Department of Virology I, National Institute of Infectious Diseases, 1-23-1 Toyama, Shinjuku-ku, Tokyo 162-8640, Japan

Y. Katakai
Corporation for Production and Research of Laboratory Primates, 1-1 Hachimandai, Tsukuba, Ibaraki 305-0843, Japan

S. Nakamura
Research Center for Animal Life Science, Shiga University of Medical Science, Seta Tsukinowa-cho, Otsu, Shiga 520-2192, Japan

Published online: 05 February 2013

Research of the long-term immune response in humans has provided several interesting parallels to the data. It was reported that complete cross-protective immunity from heterologous challenge was induced in individuals 1–2 months after a primary DENV infection, with partial immunity present up to 9 months, resulting in a milder disease of shorter duration on reinfection, and that complete serotype-specific immunity against symptomatic dengue was observed up to 18 months postinfection [30]. Guzman and Sierra have previously recorded the long-term presence of both DENV-specific antibodies and T cells up to 20 years after natural infections [10, 31]. Of note, increased T cell activation is reportedly associated with severe dengue disease [7, 8]. Thus, the balance between humoral and cellular immunity may be important in the control of dengue diseases.

However, the details regarding the implication of humoral and cellular immunity in controlling DENV infection remain to be elucidated. Previously, passive transfer of either monoclonal or polyclonal antibodies was shown to protect against homologous DENV challenge [13, 15, 16]. It was also reported that neutralizing antibodies played a greater role than cytotoxic T lymphocyte (CTL) responses in heterologous protection against secondary DENV infection *in vivo* in IFN-$\alpha/\beta R^{-/-}$ and IFN$\gamma R^{-/-}$ mouse models [18]. Moreover, $CD4^+$ T cell depletion did not affect the DENV-specific IgG or IgM Ab titers or their neutralizing activity in the IFN$\gamma R^{-/-}$ mouse model [36]. On the other hand, there are several reports showing that cellular immunity rather than humoral immunity plays an important role in the clearance of DENV. For example, in adoptive transfer experiments, although cross-reactive DENV-1-specific $CD8^+$ T cells did not mediate protection against a lethal DENV-2 infection, adoptive transfer of $CD4^+$ T cells alone mediated protection and delayed mortality in IFN-$\alpha/\beta R^{-/-}$ and IFN$\gamma R^{-/-}$ mouse models [39]. It has also been demonstrated that $CD8^+$ T lymphocytes have a direct role in protection against DENV challenge in the IFN-$\alpha/\beta R^{-/-}$ mouse model of DENV infection by depleting $CD8^+$ T cells [35]. In addition, previous data from adoptive-transfer experiments in BALB/c mice showed that cross-reactive memory $CD8^+$ T cells were preferentially activated by the secondary DENV infection, resulting in augmented IFN-γ and tumor necrosis factor-α (TNF-α) responses, and this effect was serotype-dependent [2, 3]. Although it has previously been suggested that inducing neutralizing antibodies against DENV may play an important role in controlling DENV infection, CTLs are also proposed to contribute to clearance during primary DENV infection and to pathogenesis during secondary heterologous infection in the BALB/c mouse model [4].

Why did the mouse models of DENV infection show inconsistent results *in vivo*? One of the reasons could be that these results were obtained mainly from genetically manipulated mice such as IFN-$\alpha/\beta R^{-/-}$ and IFN$\gamma R^{-/-}$ mice. Moreover, these mice were inoculated with 10^9–10^{10} genome equivalents (GE) of DENV [27, 35, 36], which were likely in large excess compared with the 10^4-10^5 GE of DENV injected into humans by a mosquito [19]. In addition, the efficiency of DENV replication in wild mice *in vivo* is very low compared to that in humans [35].

Recently, novel non-human primate models of DENV infection using rhesus macaques as well as marmosets and tamarins have been developed [24–26, 38]. An intravenous challenge of rhesus macaques with a high dose of virus inoculum (1×10^7 GE) of DENV-2 resulted in readily visible hemorrhaging, which is one of the cardinal symptoms of human DHF [26]. It was also shown that the cellular immune response was activated due to expression of IFN-γ, TNF-α, and macrophage inflammatory protein-1 β in $CD4^+$ and $CD8^+$ T cells during primary DENV infection in rhesus macaques [20]. On the other hand, in the marmoset model of DENV infection, we observed high levels of viremia (10^5–10^7 GE/ml) after subcutaneous inoculation with 10^4–10^5 plaque-forming units (PFU) of DENV-2. Moreover, we demonstrated that DENV-specific IgM and IgG were consistently detected and that the DENV-2 genome was not detected in any of these marmosets inoculated with the same DENV-2 strain used in the primary infection [24]. It is notable that while neutralizing antibody titers were at levels of 1:20-1:80 before the re-challenge inoculation, the titers increased up to 1:160-1:640 after the re-challenge inoculation [24]. These results suggested that the secondary infection with DENV-2 induced a protective humoral immunity to DENV-2 and that DENV-infected marmoset models may be useful in order to analyze the relationship between DENV replication and the dynamics of adaptive immune responses *in vivo*.

Taking these findings into consideration, we investigated the dynamics of cellular immunity in response to primary and secondary DENV infection in the marmoset model.

Materials and methods

Animals

All animal studies were conducted in accordance with protocols of experimental procedures that were approved by the Animal Welfare and Animal Care Committee of the National Institute of Infectious Diseases, Japan, and the National Institute of Biomedical Innovation, Japan. A total of six male marmosets, weighing 258–512 g, were used. Common marmosets were purchased from Clea Japan Inc.

(Tokyo, Japan) and caged singly at 27 ± 2 °C in 50 ± 10 % humidity with a 12-h light-dark cycle (lighting from 7:00 to 19:00) at Tsukuba Primate Research Center, National Institute of Biomedical Innovation, Tsukuba, Japan. Animals were fed twice a day with a standard marmoset diet (CMS-1M, CLEA Japan) supplemented with fruit, eggs and milk. Water was given ad libitum. The animals were in healthy condition and confirmed to be negative for anti-dengue-virus antibodies before inoculation with dengue virus [24].

Cells

Cell culture was performed as described previously [24]. Vero cells were cultured in minimum essential medium (MEM, Sigma) with 10 % heat-inactivated fetal bovine serum (FBS, GIBCO) and 1 % non-essential amino acid (NEAA, Sigma) at 37 °C in 5 % CO_2. C6/36 cells were cultured in MEM with 10 % FBS and 1 % NEAA at 28 °C in 5 % CO_2.

Virus

DENV type 2 (DENV-2) strain DHF0663 (accession no. AB189122) and strain D2/Hu/Maldives/77/2008NIID (Mal/77/08) were used for inoculation studies. The DENV-2, DHF0663 strain was isolated from a DHF case in Indonesia. The DENV-2 Mal/77/08 strain was isolated from imported DF cases from the Maldives. For all DENV strains, isolated clinical samples were propagated in C6/36 cells and were used within four passages on C6/36 cells. Culture supernatant from infected C6/36 cells was

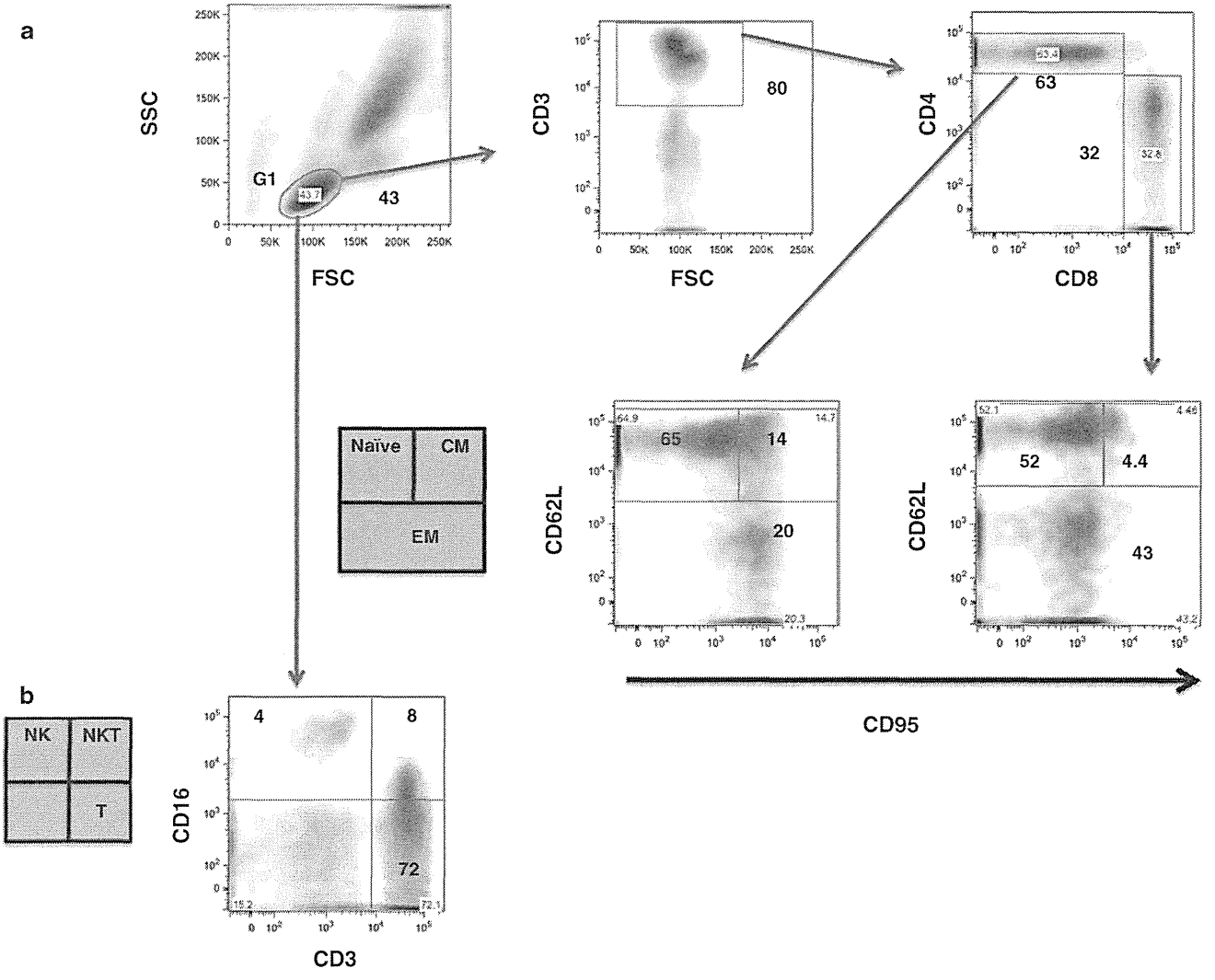

Fig. 1 Flow cytometric analysis of naïve, central/effector memory T cells and NK/NKT cells in marmosets. (**a**) Gating strategy to indentify CD4 and CD8 T, NK and NKT cells. The G1 population was selected and analyzed for CD4 and CD8 T, NK and NKT cells. (**a**) Profiling of naïve, central memory, and effector memory CD4 and CD8 T cells in total CD4 and CD8 T cells. (**b**) Profiling of NK and NKT cells in total lymphocytes. Results shown are representative of three healthy marmosets used in this study

centrifuged at 3,000 rpm for 5 min to remove cell debris and then stored at −80 °C until use.

Infection of the marmosets with DENV

In the challenge experiments, profiling of the key adaptive and innate immune cells in the marmosets after infection with DENV-2 was done. For primary DENV infection, four marmosets were inoculated subcutaneously in the back with either 1.9×10^5 PFU of the DENV-2 Mal/77/08 strain (Cj08-007, Cj07-011) or 1.8×10^4 PFU of the DHF0663 strain (Cj07-006, Cj07-008) [24]. In the case of the DENV re-challenge experiment, two marmosets initially inoculated with 1.8×10^5 PFU of the DHF0663 strain were re-inoculated 33 weeks after the primary challenge with 1.8×10^5 PFU of the same strain (Cj07-007, Cj07-014) [24]. Blood samples were collected on days 0, 1, 3, 7, 14, and 21 after inoculation and were used for virus titration and flow cytometric analysis. Inoculation with DENV and blood drawing were performed under anesthesia with 5 mg/kg of ketamine hydrochloride. Day 0 was defined as the day of virus inoculation. The viral loads in marmosets obtained in a previous study are shown in Supplementary Figure 1 [24].

Flow cytometry

Flow cytometry was performed as described previously [37]. Fifty microliters of whole blood from marmosets was stained with combinations of fluorescence-conjugated monoclonal antibodies; anti-CD3 (SP34-2; Becton Dickinson), anti-CD4 (L200; BD Pharmingen), anti-CD8 (CLB-T8/4H8; Sanquin), anti-CD16 (3G8; BD Pharmingen), anti-CD95 (DX2; BD Pharmingen), and anti-CD62L (145/15; Miltenyi Biotec). Then, erythrocytes were lysed with FACS lysing solution (Becton Dickinson). After washing with a sample buffer containing phosphate-buffered saline (PBS) and 1 % FBS, the labeled cells were resuspended in a fix buffer containing PBS and 1 % formaldehyde. The expression of these markers on the lymphocytes was analyzed using a FACSCanto II flow cytometer (Becton Dickinson). The data analysis was conducted using FlowJo software (Treestar, Inc.). Results are shown as mean ± standard deviation (SD) for the marmosets used in this study.

Table 1 Subpopulation ratios of lymphocytes in marmosets

Subpopulation name	Subpopulation ratios (Mean ± SD: %)
$CD3^+$	75.7 ± 6.4
$CD3^+CD4^+$	65.4 ± 6.8
$CD3^+CD4^+CD62L^+CD95^-$ (CD4 T_N)	65.9 ± 3.7
$CD3^+CD4^+CD62L^+CD95^+$(CD4 T_{CM})	16.4 ± 2.9
$CD3^+CD4^+CD62LCD95^\pm$ (CD4 T_{EM})	19.5 ± 2.5
$CD3^+CD8^+$	29.0 ± 8.0
$CD3^+CD8^+CD62L^+CD95^-$ (CD8 T_N)	66.7 ± 10.2
$CD3^+CD8^+CD62L^+CD95^+$(CD8 T_{CM})	4.7 ± 3.6
$CD3^+CD8^+CD62LCD95^\pm$ (CD8 T_{EM})	28.8 ± 14.8
CD3CD16 + (NK)	4.2 ± 2.6
$CD3^+CD16^+$ (NKT)	5.1 ± 3.4

SD: Standard deviation

Results shown are mean ± SD from 3 healthy marmosets

Results

Naïve central/effector memory T cells and NK/NKT cells in marmosets

Basic information regarding CD4/CD8 naïve and central/effector memory T cells and NK/NKT cells in common marmosets was unavailable. Thus, we examined the immunophenotypes of lymphocyte subsets in the marmosets (Fig. 1). The gating strategy for profiling the CD4 and CD8 T cells in the marmosets by FACS is shown in Fig. 1a. Human T cells are classically divided into three functional subsets based on their cell-surface expression of CD62L and CD95, i.e., $CD62L^+CD95^-$ naive T cells (T_N), $CD62L^+CD95^+$ central memory T cells (T_{CM}), and $CD62L^-CD95^\pm$ effector memory T cells (T_{EM}) [9, 21, 28]. In this study, $CD4^+$ and $CD8^+$ T_N, T_{CM}, and T_{EM} subpopulations were defined as $CD62L^+CD95^-$, $CD62L^+CD95^+$, and $CD62L^-CD95^\pm$, respectively (Fig. 1a and Table 1). The average ratio of $CD3^+$ T lymphocytes in the total lymphocytes of three marmosets was found to be 75.7 ± 6.4 %. The average ratio of $CD4^+$ T cells in the $CD3^+$ subset was 65.4 ± 6.8 %. The average ratios of $CD4^+$ T_N, T_{CM}, and T_{EM} cells were 65.9 ± 3.7 %, 16.4 ± 2.9 %, 19.5 ± 2.5 %, respectively. The average ratio of $CD8^+$ T cells in the $CD3^+$ subset was 29.0 ± 8.0 %. The average ratios of $CD8^+$ T_N, T_{CM}, and T_{EM} cells were 66.7 ± 10.2 %, 4.7 ± 3.6 %, 28.8 ± 14.8 %, respectively.

We recently characterized a $CD16^+$ major NK cell subset in tamarins and compared NK activity in tamarins with or without DENV infection [37, 38]. In terms of NKT cells, NK1.1 (CD161) and CD1d are generally used as markers of NKT cells [32]. However, these anti-human NK1.1 and CD1d antibodies are unlikely to cross-react with the NKT cells of the marmosets. Thus, we defined NKT cells as a population expressing both CD3 and CD16 as reported previously [14, 17]. The NK and NKT cell subsets were determined to be $CD3^-CD16^+$ and $CD3^+CD16^+$ lymphocytes in the marmosets. The average ratios of NK and NKT cell subsets in the lymphocytes were 4.2 ± 2.6 % and 5.1 ± 3.4 %, respectively (Table 1). We observed that the proportions of the major lymphocyte

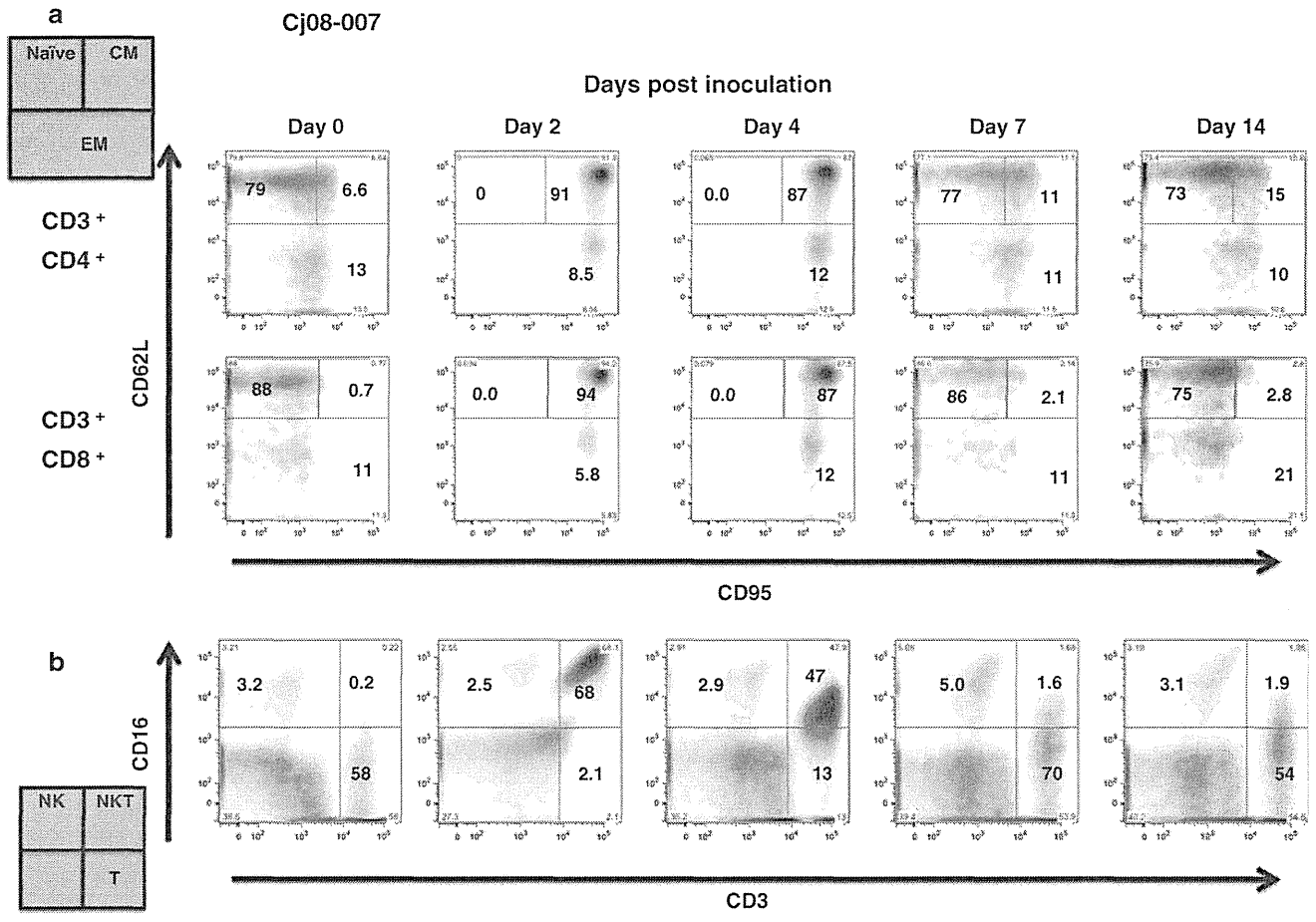

Fig. 2 Profiling of CD4 and CD8 T, NK and NKT cells in marmosets with primary infection with the DENV-2 Mal/77/08 strain. For primary DENV infection, two marmosets were inoculated subcutaneously in the back with 1.9×10^5 PFU of the DENV-2 Mal/77/08 strain. (**a**) Profiling of naïve, central memory, and effector memory CD4 and CD8 T cells in total CD4 and CD8 T cells. (**b**) Profiling of NK and NKT cells in total lymphocytes. (**a-b**) Cj08-007

subsets in the marmosets were similar to those in cynomolgus monkeys and tamarins [37, 38].

Profiling of CD4 and CD8 T, NK and NKT cells in marmosets after primary infection with DENV-2 (Mal/77/08 strain)

We investigated the cellular immune responses against DENV-2 DF strain (Mal/77/08) in marmosets. Dengue vRNA was detected in plasma samples from two marmosets on day 2 postinfection (Supplementary Fig. 1a). For the two marmosets (Cj08-007, Cj07-011), the plasma levels of vRNA reached their peaks at 9.6×10^6 and 7.0×10^6 GE/ml, respectively, on day 4 postinfection. Plasma vRNA was detected in both marmosets on days 2, 4, and 7. We then examined the profiles and frequencies of the CD4 and CD8 T, NK and NKT cells in the infected marmosets (Figs. 2–3 and Table 2). $CD4^+$ T_{CM} cells drastically increased to 88.7 ± 2.8 % from 13 ± 0.4 % between day 0 and day 2 post-inoculation (Table 2). Reciprocally, $CD4^+$ T_N cells decreased to 1.6 ± 3.3 % from 74.1 ± 0.9 % at the same time. $CD4^+$ T_{EM} cells maintained the initial levels throughout the observation period. $CD8^+$ T_{CM} cells increased to 91.9 ± 5.5 % from 2.1 ± 0.8 % between day 0 day 2 post-inoculation, and reciprocally, $CD8^+$ T_N cells decreased to 2.5 ± 4.7 % from 89.9 ± 2.5 % at the same time. In addition, NK cells maintained their initial levels throughout the observation period. However, NKT cells drastically increased to 52.6 ± 17 % from 0.2 ± 0.0 % between day 0 and day 2 post-inoculation. These results suggest that CD4/CD8 T and NKT cells may efficiently respond to the Mal/77/08 strain of DENV.

Profiling of CD4 and CD8 T, NK and NKT cells in the marmosets after primary infection with DENV-2 (DHF0663 strain)

Next, we investigated cellular immune responses against another DENV-2 DHF strain (DHF0663) in marmosets.

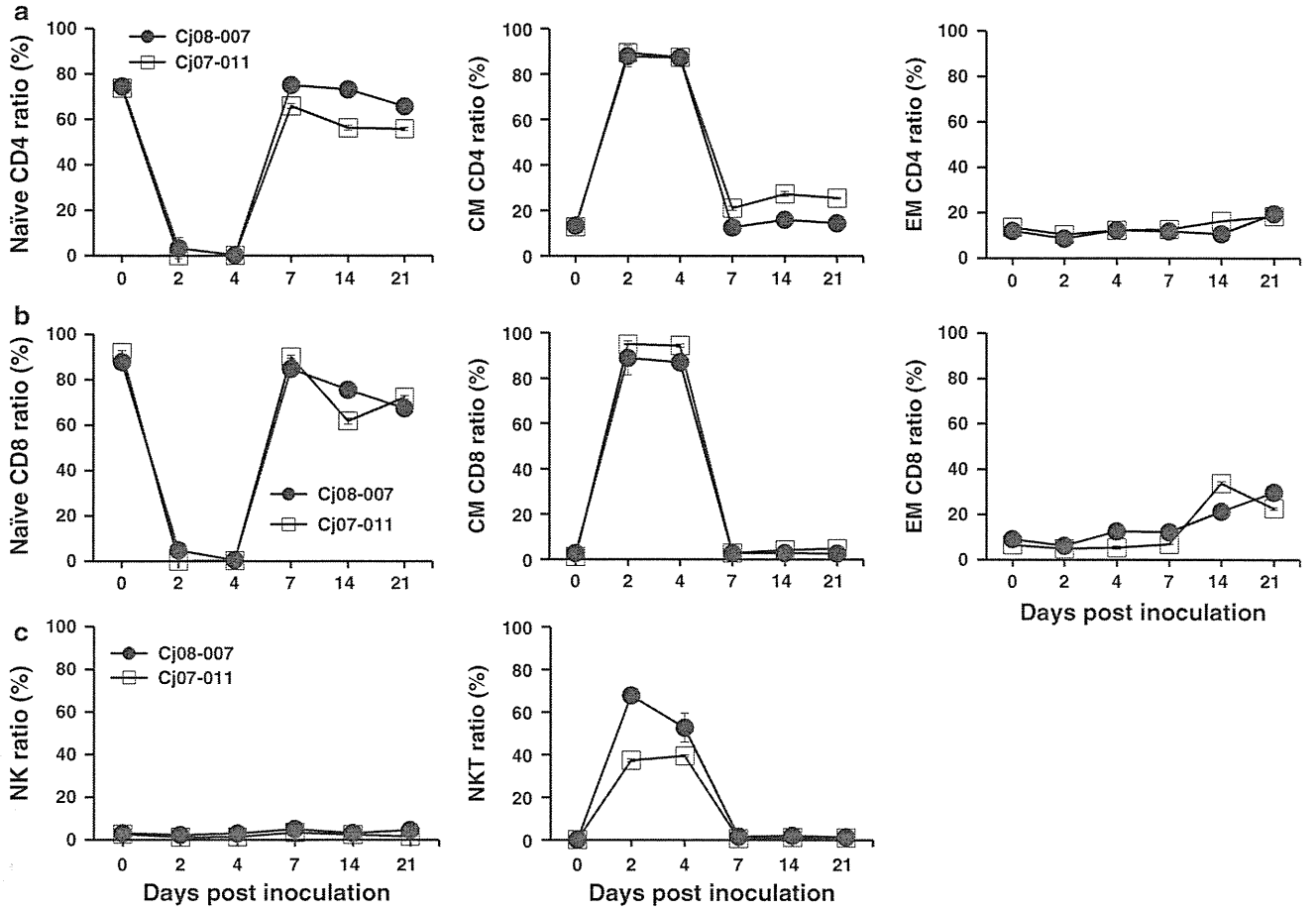

Fig. 3 Frequency of CD4 and CD8 T, NK and NKT cells in marmosets with primary infection with the DENV-2 Mal/77/08 strain. For primary DENV infection, two marmosets were inoculated subcutaneously in the back with 1.9×10^5 PFU of the DENV-2 Mal/77/08 strain. (**a**) Ratios of naïve, central memory, and effector memory CD4 T cells in total CD4 T cells. (**b**) Ratios of naïve, central memory, and effector memory CD8 T cells in total CD8 T cells. (**c**) Ratios of NK and NKT cells in total lymphocytes. (**a**-**c**) Cj08-007, Cj07-011

Table 2 Subpopulation ratios of lymphocytes in marmosets during primary DENV infection (Mal/77/08)

Subpopulation name		Subpopulation ratio (Mean ± SD: %)					
		Days after inoculation					
		Day 0	Day 2	Day 4	Day 7	Day 14	Day 21
$CD3^+CD4^+CD62L^+CD95''$	($CD4\ T_N$)	74.1 ± 0.9	1.6 ± 3.3	0.2 ± 0.3	70.5 ± 5.5	64.8 ± 9.7	60.8 ± 5.9
$CD3^+CD4^+CD62L^+CD95^+$	($CD4\ T_{CM}$)	13 ± 0.4	88.7 ± 2.8	87.4 ± 0.2	16.8 ± 5.0	21.6 ± 6.5	20 ± 6.4
$CD3^+CD4^+CD62LCD95^\pm$	($CD4\ T_{EN}$)	12.8 ± 0.9	9.5 ± 1.0	12.3 ± 0.4	12.3 ± 0.5	134 ± 3.2	189 ± 1.4
$CD3^+CD8^+CD62L^+CD95^-$	($CD8\ T_N$)	89.9 ± 2.5	2.5 ± 4.7	0.3 ± 0.3	87.5 ± 3.3	68.7 ± 79	69.8 ± 3.1
$CD3^+CD8^+CD62L^+CD95^+$	($CD8\ T_{CM}$)	2.1 ± 0.8	91.9 ± 5.5	90.6 ± 4.2	2.8 ± 0.5	3.5 ± 08	3.8 ± 1.2
$CD3^+CD8^+CD62LCD95^\pm$	($CD8\ T_{EN}$)	7.8 ± 1.6	5.6 ± 0.8	9.0 ± 4.1	9.5 ± 3.1	27.6 ± 72	26.3 ± 4.3
$CD3^-CD16+$	(NK)	2.9 ± 0.2	1.8 ± 0.6	2.2 ± 0.9	4.2 ± 0.9	2.8 ± 04	3.2 ± 1.7
$CD3^+CD16^+$	(NKT)	0.2 ± 0.0	52.6 ± 17	46.1 ± 8.5	1.1 ± 05	1.7 ± 05	1.2 ± 0.2

SD: Standard deviation

Results shown are mean ± SD from two marmosets as shown in Figure 3

Dengue vRNA was detected in plasma samples from the marmosets on day 2 post-infection ([24], Supplementary Fig. 1b). For the two marmosets (Cj07-006, Cj07-008), the plasma vRNA levels were found to be 3.4×10^5 and 3.8×10^5 GE/ml on day 2 and 2.0×10^6 and 9.4×10^5 GE/ml, respectively, at the peak on day 4 post-infection and became undetectable by day 14. Thus, we examined the profiles and frequencies of the $CD4^+$ and $CD8^+$ T, NK and NKT cells in these DENV-infected marmosets (Fig. 4–5 and Table 3). It was found that on day 7 post-inoculation, $CD4^+$ and $CD8^+$ T_N cells decreased, and in contrast, the T_{CM} populations increased in both marmosets; however, the changes in proportion were much less pronounced than in the case of the marmosets infected with the DF strain. We observed no consistent tendency in the kinetics of $CD4^+$ and $CD8^+$ T_{EM} cells nor in NK and NKT cells. These results suggest that the strength of T cell responses may be dependent on the strain of DENV.

Profiling of CD4 and CD8 T, NK and NKT cells in marmosets re-challenged with a DENV-2 strain

In order to examine the cellular immune responses against re-challenge with a DENV-2 DHF strain in the marmoset model, marmosets were infected twice with the same DENV-2 strain (DHF0663) with an interval of 33 weeks after the primary infection. The results showed that vRNA and NS1 antigens were not detected in plasma and that the neutralizing antibody titer was obviously increased after the secondary infection. The data indicated that the primary infection induced protective immunity, including a neutralizing antibody response to re-challenge with the same DENV strain ([24]; Supplementary Fig. 1c). We also investigated the profiles of the CD4 and CD8 T, NK and NKT cells in the marmosets (Cj07-007, Cj07-014) that were re-challenged with the same DENV-2 strain (DHF0663) (Figs. 6–7). $CD4^+$ T_{CM} cells drastically increased on day 14 post-inoculation. On the other hand,

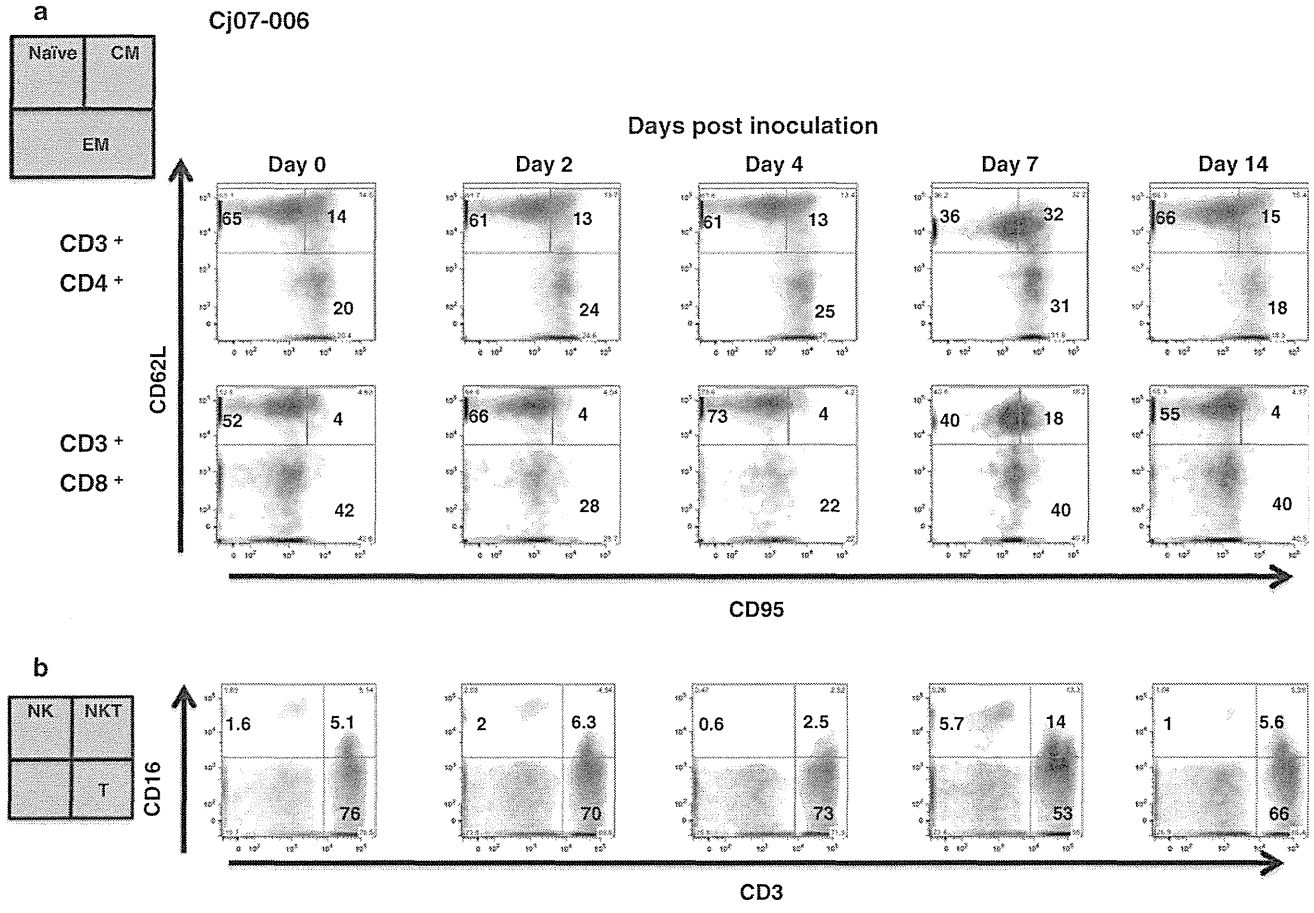

Fig. 4 Profiling of CD4 and CD8 T, NK and NKT cells in marmosets with primary infection with the DENV-2 DHF0663 strain. For primary DENV infection, two marmosets were inoculated subcutaneously in the back with 1.8×10^4 PFU of the DENV-2 DHF0663 strain. (**a**) Profiling of naïve, central memory, and effector memory CD4 and CD8 T cells in total CD4 and CD8 T cells. (**b**) Profiling of NK and NKT cells in total lymphocytes. (**a-b**) Cj07-006

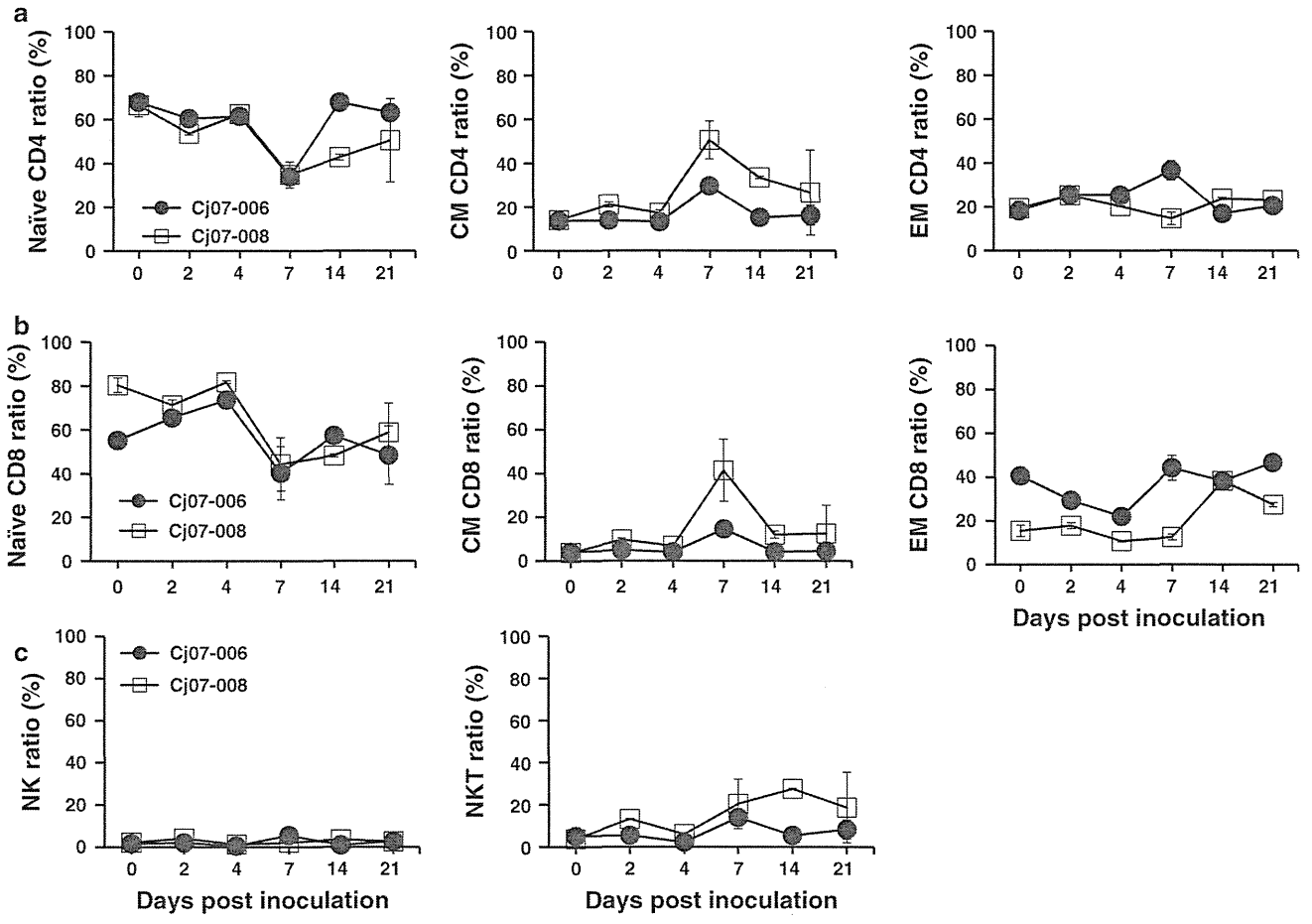

Fig. 5 Frequency of CD4 and CD8 T, NK and NKT cells in marmosets with primary infection with the DENV-2 DHF0663 strain. For primary DENV infection, two marmosets were inoculated subcutaneously in the back with 1.8×10^4 PFU of the DENV-2 DHF0663 strain. (**a**) Ratios of naïve, central memory, and effector memory CD4 T cells in total CD4 T cells. (**b**) Ratios of naïve, central memory, and effector memory CD8 T cells in total CD8 T cells. (**c**) Ratios of NK and NKT cells in total lymphocytes. (**a**-**c**) Cj07-006, Cj07-008

Table 3 Subpopulation ratios of lymphocytes in marmosets during primary DENV infection (DHF0663)

Subpopulation name		Subpopulation ratios (Mean ± SD: %)					
		Days after inoculation					
		Day 0	Day 2	Day 4	Day 7	Day1 4	Day 21
$CD3^+CD4^+CD62L^+CD95^-$	($CD4\ T_N$)	67.3 ± 3.6	57.0 ± 4.0	61.9 ± 0.9	34.4 ± 3.6	55.2 ± 14	56.7 ± 13
$CD3^+CD4^+CD62L^+CD95^+$	($CD4T_{CM}$)	13.9 ± 1.3	17.5 ± 4.1	15.2 ± 2.5	40.0 ± 13	33.8 ± 10	21.3 ± 12
$CD3^+CD8^+CD62L^-CD95^{\pm}$	($CD4\ T_{EM}$)	18.8 ± 2.2	25.3 ± 0.9	22.8 ± 2.9	25.6 ± 13	20.3 ± 4.0	21.8 ± 1.5
$CD3^+CD8^+CD62L^+CD95^-$	($CDS\ T_N$)	67.8 ± 14	68.4 ± 3.7	77.7 ± 4.6	42.2 ± 7.4	52.7 ± 5.5	53.5 ± 9.8
$CD3^+CD8^+CD62L^+CD95^-$	($CDS\ T_{CM}$)	3.9 ± 0.6	7.4 ± 2.8	5.5 ± 1.6	28 ± 17	8.1 ± 4.6	8.6 ± 8.9
$CD3^+CD8^+CD62L^-CD95^{\pm}$	($CDS\ T_{EM}$)	28 ± 14	23.5 ± 6.7	16.4 ± 6.5	28.3 ± 18	38.2 ± 1.9	37.0 ± 11
$CD3^-CD16^+$	(NK)	4.7 ± 1.0	4.2 ± 1.9	2.0 ± 1.1	6.3 ± 2.3	5.1 ± 2.2	7.3 ± 1.2
$CD3^+CD16^+$	(NKT)	7.8 ± 1.0	9.3 ± 4.5	5.9 ± 2.6	22.6 ± 8.4	20.6 ± 10	17.3 ± 10

SD: Standard deviation

Results shown are mean ± SD from 2 marmosets as shown in Figure 5

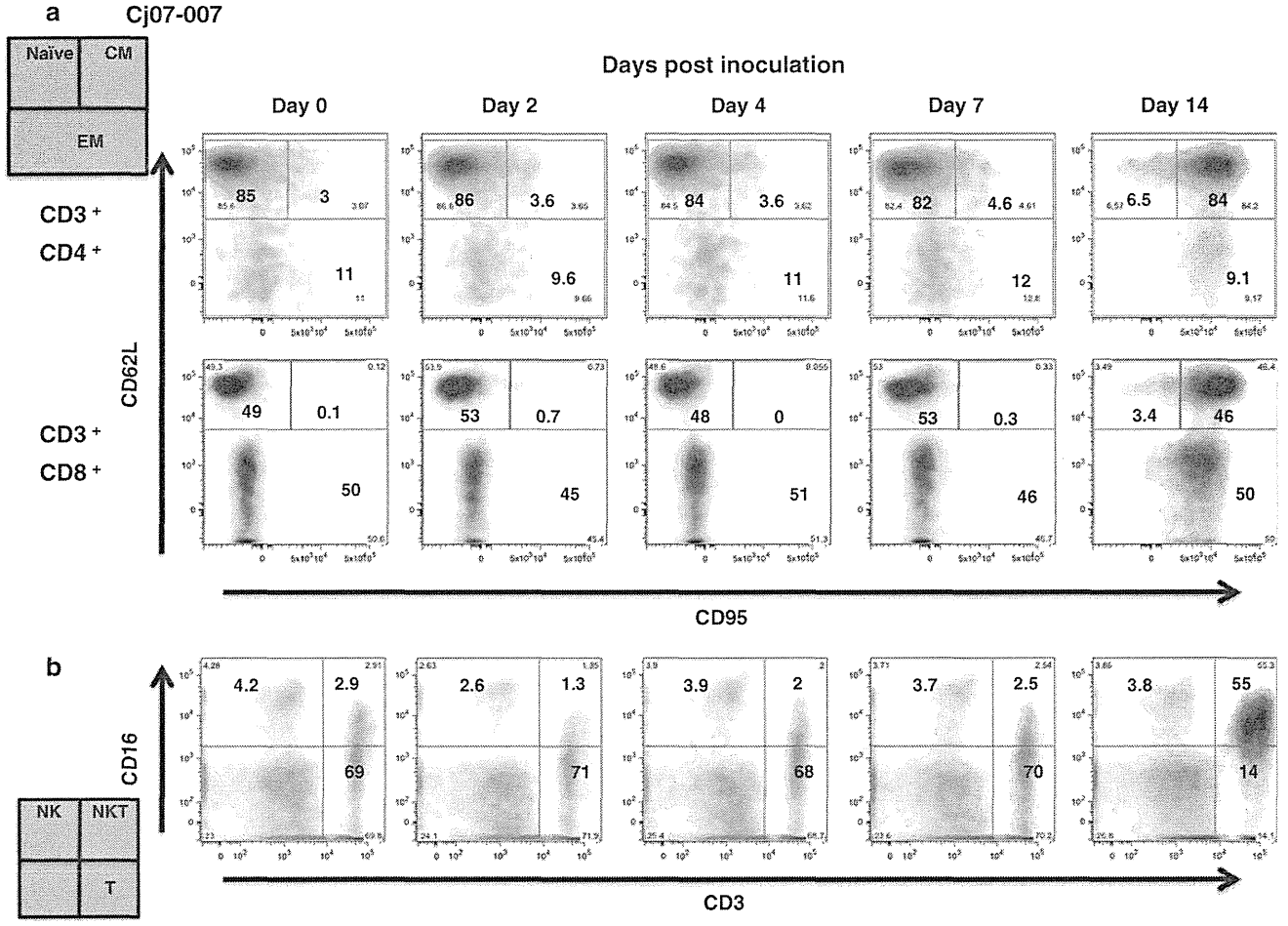

Fig. 6 Profiling of CD4 and CD8 T, NK and NKT cells in marmosets after re-challenge with the DENV-2 DHF0663 strain. Two marmosets that were initially inoculated with 1.8×10^5 PFU of the DHF0663 strain were re-inoculated 33 weeks after the primary challenge with 1.8×10^5 PFU of the same strain. (**a**) Profiling of naïve, central memory, and effector memory CD4 and CD8 T cells in total CD4 and CD8 T cells. (**b**) Profiling of NK and NKT cells in total lymphocytes. (**a-b**) Cj07-007

$CD4^+$ T_N cells decreased strongly at the same time. $CD4^+$ T_{EM} cells maintained their initial levels through the observation period. Similarly, $CD8^+$ T_{CM} and NKT cells clearly increased on day 14 post-inoculation. Importantly, these T cell responses were induced one week after the obvious induction of the neutralizing antibody in the marmosets [24]. These results suggest that the neutralizing antibody may play a critical role in the complete inhibition of the secondary DENV infection.

Discussion

In this study, we demonstrated the dynamics of the central/effector memory T cells and NK/NKT subsets against DENV infection in our marmoset model. First, we characterized the central/effector memory T and NK/NKT subsets in marmosets (Fig. 1). Second, we found that CD4/CD8 central memory T cells and NKT cells had significant responses in the primary DENV infection, and the levels appeared to be dependent on the strain of the virus employed for challenge experiments (Figs. 2–5). Finally, we found delayed responses of CD4/CD8 central memory T cells in the monkeys re-challenged with the same DENV DHF strain, despite the complete inhibition of DENV replication (Figs. 6–7).

The present study shed light on the dynamics of cellular and humoral immune responses against DENV *in vivo* in the marmoset model. Our results showed that cellular immune responses were induced earlier than antibody responses in the primary infection. Thus, our results suggest the possibility that cellular immunity may contribute, at least in part, to the control of primary DENV infection. On the other hand, in the presence of neutralizing antibodies in the re-challenged monkeys [24], delayed (on day 14 after the re-challenge) responses of CD4/CD8 central memory T cells were observed despite the complete inhibition of DENV replication. These results indicate that

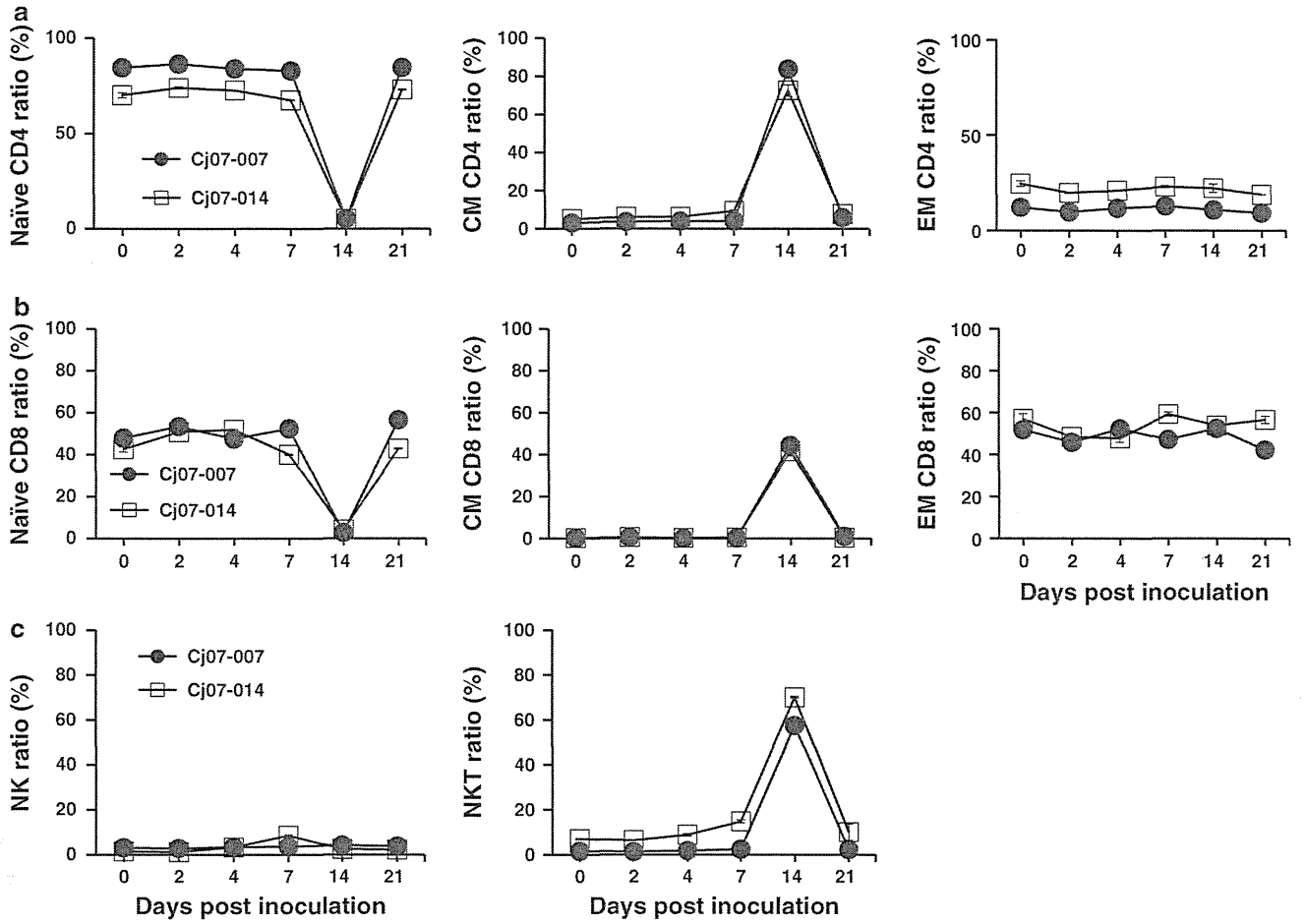

Fig. 7 Frequency of CD4 and CD8 T, NK and NKT cells in marmosets after re-challenge with the DENV-2 DHF0663 strain. Two marmosets initially inoculated with 1.8×10^5 PFU of the DHF0663 strain were re-inoculated 33 weeks after the primary challenge with 1.8×10^5 PFU of the same strain. (**a**) Ratios of naïve, central memory, and effector memory CD4 T cells in total CD4 T cells. (**b**) Ratios of naïve, central memory, and effector memory CD8 T cells in total CD8 T cells. (**c**) Ratios of NK and NKT cells in total lymphocytes. (**a**-**c**) Cj07-007, Cj07-014

cellular immunity is unlikely to play a major role in the control of DENV re-infection. Alternatively, it is still possible that components of cellular immunity, such as memory T cells, could partially play a helper role for the enhanced induction of neutralizing antibodies even without an apparent increase in the proportion of T_{CM}, resulting in efficient prevention of DENV replication.

It is possible that the DENV strains used in this study influence the strength of cellular immune responses. The differences in cellular immune responses between the monkeys infected with the DF and DHF strains are probably not caused by individual differences in the marmosets, because the FACS results were consistent with each pair of marmosets. It was shown previously that there was a reduction in CD3, CD4, and CD8 cells in DHF and that lower levels of CD3, CD4, and CD8 cells discriminated DHF from DF patients during the febrile stage of illness [5]. There was a significant increase in an early activation marker on $CD8^+$ T cells in children with DHF compared with DF during the febrile period of illness [8]. Another group reported that levels of peripheral blood mononuclear cell apoptosis were higher in children developing DHF [23]. Moreover, cDNA array and ELISA screening demonstrated that IFN-inducible genes, IFN-induced genes and IFN production were strongly up-regulated in DF patients when compared to DHF patients, suggesting a significant role of the IFN system during infection with DF strains when compared to DHF strains [34]. Thus, it is reasonable to assume that DHF strains might have the ability to negatively regulate T cell responses. A recent report demonstrating that the sequence of a DHF strain differed from that of a DF strain at six unique amino acid residues located in the membrane, envelope and non-structural genes [33], which supports our notion.

Alternatively, another possibility is that the strength of T cell responses might depend on the viral load. In fact, in

our results, the stronger T cell responses in monkeys infected with the DF strain were paralleled by higher viral loads, which was in contrast to the result obtained with DHF-strain-infected animals with lower viral loads. Of note, the tenfold higher challenge dose of the DF strain used in this study (1.9×10^5 PFU) compared to the DHF strain (1.8×10^4 PFU) could have simply led to tenfold higher peak viral RNA levels in monkeys infected with the DF strain. In either case, the relationship between the strength of the antiviral immune response and the viral strain remains to be elucidated. Further *in vivo* characterization of the antiviral immunity and the viral replication kinetics induced by infection with various DENV strains isolated from DF and DHF patients will help to understand the mechanism of differential disease progression in the course of DENV infection.

We observed that dengue vRNA was not detected in plasma samples from marmosets re-infected with the same DENV-2 DHF strain 33 weeks after the primary infection. This result suggests that memory B cells induced in the primary DENV infection were predominantly activated to produce neutralizing antibodies against the same DHF strain in the secondary infection in the absence of apparent cellular immune responses. A previous report showed that DENV infection induces a high-titered neutralizing antibody that can provide long-term immunity to the homologous DENV serotype [22], which is consistent with our results. By contrast, the role of cellular immune responses in the control of DENV infection remains to be elucidated. Our results in this study may suggest that cellular immune responses and neutralizing antibodies acted cooperatively to control primary DENV infection. In DENV-infected patients, it may be difficult to distinguish whether each case is primary or secondary DENV infection and also to serially collect blood samples for immunological study in the course of the infection, which is likely to be the reason for the discrepancy regarding the importance of cellular immunity in DENV infection. From this point of view, our marmoset model of DENV infection will further provide important information regarding the role of cellular immune responses in DENV infection.

Acknowledgments We would like to give special thanks to members of The Corporation for Production and Research of Laboratory Primates for technical assistance. We also appreciate Ms. Tomoko Ikoma and Mizuho Fujita for technical assistance. This work was supported by grants from the Ministry of Health, Labor and Welfare of Japan, and by the Environment Research and Technology Development Fund (D-1007) from the Ministry of the Environment of Japan.

Conflict of interest The authors declare that the research was conducted in the absence of any commercial or financial relationships that could be construed as a potential conflict of interest.

References

1. Balsitis SJ, Williams KL, Lachica R, Flores D, Kyle JL, Mehlhop E, Johnson S, Diamond MS, Beatty PR, Harris E (2010) Lethal antibody enhancement of dengue disease in mice is prevented by Fc modification. PLoS Pathog 6:e1000790
2. Beaumier CM, Mathew A, Bashyam HS, Rothman AL (2008) Cross-reactive memory CD8(+) T cells alter the immune response to heterologous secondary dengue virus infections in mice in a sequence-specific manner. J Infect Dis 197:608–617
3. Beaumier CM, Rothman AL (2009) Cross-reactive memory CD4+ T cells alter the CD8+ T-cell response to heterologous secondary dengue virus infections in mice in a sequence-specific manner. Viral Immunol 22:215–219
4. Beaumier CM, Jaiswal S, West KY, Friberg H, Mathew A, Rothman AL (2010) Differential in vivo clearance and response to secondary heterologous infections by H2(b)-restricted dengue virus-specific CD8+ T cells. Viral Immunol 23:477–485
5. Fadilah SA, Sahrir S, Raymond AA, Cheong SK, Aziz JA, Sivagengei K (1999) Quantitation of T lymphocyte subsets helps to distinguish dengue hemorrhagic fever from classic dengue fever during the acute febrile stage. Southeast Asian J Trop Med Public Health 30:710–717
6. Goncalvez AP, Engle RE, St Claire M, Purcell RH, Lai CJ (2007) Monoclonal antibody-mediated enhancement of dengue virus infection in vitro and in vivo and strategies for prevention. Proc Natl Acad Sci USA 104:9422–9427
7. Green S, Pichyangkul S, Vaughn DW, Kalayanarooj S, Nimmannitya S, Nisalak A, Kurane I, Rothman AL, Ennis FA (1999) Early CD69 expression on peripheral blood lymphocytes from children with dengue hemorrhagic fever. J Infect Dis 180: 1429–1435
8. Green S, Vaughn DW, Kalayanarooj S, Nimmannitya S, Suntayakorn S, Nisalak A, Lew R, Innis BL, Kurane I, Rothman AL, Ennis FA (1999) Early immune activation in acute dengue illness is related to development of plasma leakage and disease severity. J Infect Dis 179:755–762
9. Gupta S, Gollapudi S (2008) CD95-mediated apoptosis in naive, central and effector memory subsets of CD4+ and CD8+ T cells in aged humans. Exp Gerontol 43:266–274
10. Guzman MG, Alvarez M, Rodriguez-Roche R, Bernardo L, Montes T, Vazquez S, Morier L, Alvarez A, Gould EA, Kouri G, Halstead SB (2007) Neutralizing antibodies after infection with dengue 1 virus. Emerg Infect Dis 13:282–286
11. Halstead SB (1979) In vivo enhancement of dengue virus infection in rhesus monkeys by passively transferred antibody. J Infect Dis 140:527–533
12. Halstead SB (2007) Dengue. Lancet 370:1644–1652
13. Henchal EA, Henchal LS, Schlesinger JJ (1988) Synergistic interactions of anti-NS1 monoclonal antibodies protect passively immunized mice from lethal challenge with dengue 2 virus. J Gen Virol 69(Pt 8):2101–2107
14. Hus I, Staroslawska E, Bojarska-Junak A, Dobrzynska-Rutkowska A, Surdacka A, Wdowiak P, Wasiak M, Kusz M, Twardosz A, Dmoszynska A, Rolinski J (2011) CD3+/CD16+CD56+ cell numbers in peripheral blood are correlated with higher tumor burden in patients with diffuse large B-cell lymphoma. Folia Histochem Cytobiol 49:183–187
15. Kaufman BM, Summers PL, Dubois DR, Eckels KH (1987) Monoclonal antibodies against dengue 2 virus E-glycoprotein protect mice against lethal dengue infection. Am J Trop Med Hyg 36:427–434
16. Kaufman BM, Summers PL, Dubois DR, Cohen WH, Gentry MK, Timchak RL, Burke DS, Eckels KH (1989) Monoclonal

antibodies for dengue virus prM glycoprotein protect mice against lethal dengue infection. Am J Trop Med Hyg 41:576–580
17. Khvedelidze M, Chkhartishvili N, Abashidze L, Dzigua L, Tsertsvadze T (2008) Expansion of CD3/CD16/CD56 positive NKT cells in HIV/AIDS: the pilot study. Georgian Med News 165:78–83
18. Kyle JL, Balsitis SJ, Zhang L, Beatty PR, Harris E (2008) Antibodies play a greater role than immune cells in heterologous protection against secondary dengue virus infection in a mouse model. Virology 380:296–303
19. Mathew A, Rothman AL (2008) Understanding the contribution of cellular immunity to dengue disease pathogenesis. Immunol Rev 225:300–313
20. Mladinich KM, Piaskowski SM, Rudersdorf R, Eernisse CM, Weisgrau KL, Martins MA, Furlott JR, Partidos CD, Brewoo JN, Osorio JE, Wilson NA, Rakasz EG, Watkins DI (2012) Dengue virus-specific CD4+ and CD8+ T lymphocytes target NS1, NS3 and NS5 in infected Indian rhesus macaques. Immunogenetics 64:111–121
21. Mueller YM, Makar V, Bojczuk PM, Witek J, Katsikis PD (2003) IL-15 enhances the function and inhibits CD95/Fas-induced apoptosis of human CD4+ and CD8+ effector-memory T cells. Int Immunol 15:49–58
22. Murphy BR, Whitehead SS (2011) Immune response to dengue virus and prospects for a vaccine. Annu Rev Immunol 29:587–619
23. Myint KS, Endy TP, Mongkolsirichaikul D, Manomuth C, Kalayanarooj S, Vaughn DW, Nisalak A, Green S, Rothman AL, Ennis FA, Libraty DH (2006) Cellular immune activation in children with acute dengue virus infections is modulated by apoptosis. J Infect Dis 194:600–607
24. Omatsu T, Moi ML, Hirayama T, Takasaki T, Nakamura S, Tajima S, Ito M, Yoshida T, Saito A, Katakai Y, Akari H, Kurane I (2011) Common marmoset (Callithrix jacchus) as a primate model of dengue virus infection: development of high levels of viremia and demonstration of protective immunity. J Gen Virol 92:2272–2280
25. Omatsu T, Moi ML, Takasaki T, Nakamura S, Katakai Y, Tajima S, Ito M, Yoshida T, Saito A, Akari H, Kurane I (2013) Changes in hematological and serum biochemical parameters in common marmosets (Cllithrix jacchus) after inoculation with dengue virus. J Med Primatol 54:89–98
26. Onlamoon N, Noisakran S, Hsiao HM, Duncan A, Villinger F, Ansari AA, Perng GC (2010) Dengue virus-induced hemorrhage in a nonhuman primate model. Blood 115:1823–1834
27. Pawitan JA (2011) Dengue virus infection: predictors for severe dengue. Acta Med Indones 43:129–135
28. Pitcher CJ, Hagen SI, Walker JM, Lum R, Mitchell BL, Maino VC, Axthelm MK, Picker LJ (2002) Development and homeostasis of T cell memory in rhesus macaque. J Immunol 168:29–43
29. Rigau-Perez JG, Clark GG, Gubler DJ, Reiter P, Sanders EJ, Vorndam AV (1998) Dengue and dengue haemorrhagic fever. Lancet 352:971–977
30. Sabin AB (1950) The dengue group of viruses and its family relationships. Bacteriol Rev 14:225–232
31. Sierra B, Garcia G, Perez AB, Morier L, Rodriguez R, Alvarez M, Guzman MG (2002) Long-term memory cellular immune response to dengue virus after a natural primary infection. Int J Infect Dis 6:125–128
32. Terabe M, Berzofsky JA (2008) The role of NKT cells in tumor immunity. Adv Cancer Res 101:277–348
33. Tuiskunen A, Monteil V, Plumet S, Boubis L, Wahlstrom M, Duong V, Buchy P, Lundkvist A, Tolou H, Leparc-Goffart I (2011) Phenotypic and genotypic characterization of dengue virus isolates differentiates dengue fever and dengue hemorrhagic fever from dengue shock syndrome. Arch Virol 156:2023–2032
34. Ubol S, Masrinoul P, Chaijaruwanich J, Kalayanarooj S, Charoensirisuthikul T, Kasisith J (2008) Differences in global gene expression in peripheral blood mononuclear cells indicate a significant role of the innate responses in progression of dengue fever but not dengue hemorrhagic fever. J Infect Dis 197:1459–1467
35. Yauch LE, Zellweger RM, Kotturi MF, Qutubuddin A, Sidney J, Peters B, Prestwood TR, Sette A, Shresta S (2009) A protective role for dengue virus-specific CD8+ T cells. J Immunol 182:4865–4873
36. Yauch LE, Prestwood TR, May MM, Morar MM, Zellweger RM, Peters B, Sette A, Shresta S (2010) CD4+ T cells are not required for the induction of dengue virus-specific CD8+ T cell or antibody responses but contribute to protection after vaccination. J Immunol 185:5405–5416
37. Yoshida T, Saito A, Iwasaki Y, Iijima S, Kurosawa T, Katakai Y, Yasutomi Y, Reimann KA, Hayakawa T, Akari H (2010) Characterization of natural killer cells in tamarins: a technical basis for studies of innate immunity. Front Microbiol 1:128
38. Yoshida T, Omatsu T, Saito A, Katakai Y, Iwasaki Y, Iijima S, Kurosawa T, Hamano M, Nakamura S, Takasaki T, Yasutomi Y, Kurane I, Akari H (2012) CD16(+) natural killer cells play a limited role against primary dengue virus infection in tamarins. Arch Virol 157:363–368
39. Zompi S, Santich BH, Beatty PR, Harris E (2012) Protection from secondary dengue virus infection in a mouse model reveals the role of serotype cross-reactive B and T cells. J Immunol 188:404–416